The Plant Cell, Vol. 31: 2711–2733, November 2019, www.plantcell.org © 2019 ASPB.

Diurnal Regulation of Plant Epidermal Wax Synthesis through Antagonistic Roles of the Transcription Factors SPL9 and DEWAX

Rong-Jun Li,[a,b,1] Lin-Mao Li,[a,c,d,1] Xiu-Lin Liu,[a,c] Jang-Chol Kim,[d] Matthew A. Jenks,[e] and Shiyou Lü[f,2]

[a] Key Laboratory of Plant Germplasm Enhancement and Specialty Agriculture, Wuhan Botanical Garden, Chinese Academy of Sciences, Wuhan 430074, China
[b] Sino-Africa Joint Research Center, Chinese Academy of Sciences, Wuhan, 430074, China
[c] University of Chinese Academy of Sciences, Beijing 100049, China
[d] College of Life Sciences, Wuhan University, Wuhan 430072, China
[e] School of Plant Sciences, College of Agriculture and Life Sciences, The University of Arizona, Tucson, Arizona 85721
[f] State Key Laboratory of Biocatalysis and Enzyme Engineering, School of Life Sciences, Hubei University, Wuhan, 434200, China

ORCID IDs: 0000-0001-5684-7583 (R.-J.L.); 0000-0003-0330-917X (L.-M.L.); 0000-0002-8940-8162 (X.-L.L.); 0000-0001-6446-673X (J.-C.K.); 0000-0003-1134-3925 (M.A.J.); 0000-0003-0449-2471 (S.L.)

Plant surface waxes form an outer barrier that protects the plant from many forms of environmental stress. The deposition of cuticular waxes on the plant surface is regulated by external environmental changes, including light and dark cycles. However, the underlying molecular mechanisms controlling light regulation of wax production are still poorly understood, especially at the posttranscriptional level. In this paper, we report the regulation of cuticular wax production by the miR156-SPL9 (SQUAMOSA PROMOTER BINDING PROTEIN-LIKE 9) module in Arabidopsis (*Arabidopsis thaliana*). When compared with wild-type plants, miR156 and *SPL9* mutants showed significantly altered cuticular wax amounts in both stems and leaves. Furthermore, it was found that SPL9 positively regulates gene expression of the alkane-forming enzyme *ECERIFERUM1* (*CER1*), as well as the primary (1-) alcohol-forming enzyme *ECERIFERUM4* (*CER4*), to enhance alkane and 1-alcohol synthesis, respectively. Our results indicate that complex formation of SPL9 with a negative regulator of wax synthesis, DEWAX, will hamper SPL9 DNA binding ability, possibly by interfering with SPL9 homodimerization. Combined with their diurnal gene and protein expressions, this dynamic repression–activation transcriptional module defines a dynamic mechanism that may allow plants to optimize wax synthesis during daily cycles. These findings provide a regulatory framework for environmental signal integration in the regulation of wax synthesis.

INTRODUCTION

The surface of most aerial plant organs is covered with a coating of cuticular waxes that provides protection against multiple stress factors. Cuticular wax formation is tightly regulated by both developmental and environmental cues, which allows plants to adapt to changing environmental conditions during their life cycle (Shepherd and Wynne Griffiths, 2006; Samuels et al., 2008). For example, multiple plant species show higher cuticular wax synthesis in the light than in the dark (Baker, 1974; Giese, 1975; Shepherd et al., 1995; Go et al., 2014). However, it is unclear how wax synthesis is activated by light; nor is it clear whether light induction of wax functions as a beneficial environmental adaptation or as a developmental regulator (Shepherd and Wynne Griffiths, 2006).

Cuticular waxes comprise an admixture of very-long chain aliphatic compounds including primary alcohols, alkyl esters, alkanes, ketones, aldehydes, and secondary alcohols, which are mainly synthesized in the endoplasmic reticulum (ER; Bernard and Joubès 2013). Through characterizing the wax-deficient mutants and analyzing the transcriptome of stem epidermal peels, cuticular wax biosynthetic pathways in the model plant Arabidopsis (*Arabidopsis thaliana*) have been extensively studied (Jenks et al., 1995; Suh et al., 2005; Nawrath et al., 2013). In the epidermal cells, the wax precursor very long chain fatty acids (VLCFAs) are synthesized in serial pathways. First, C16 or C18 fatty acids are synthesized in the plastid from acetyl-CoA. Second, these LCFAs are converted to LCFA-CoAs by long chain acyl-CoA synthetases and then further elongated into VLCFA-CoAs (24 to 34 carbons in length) in the ER through fatty acid elongase (Bernard and Joubès 2013). Third, different classes of cuticular wax component are further produced from VLCFA-CoAs through enzymes either involved in the alkane-forming pathway or the alcohol-forming pathway (Aarts et al., 1995; Hannoufa et al., 1996; Rowland et al., 2006; Li et al., 2008). Finally, wax compounds are transported to the plasma membrane and secreted outside cells, and then deposited on the epidermis (Bernard and Joubès 2013).

Cuticular wax metabolic pathways are under a substantial amount of transcriptional regulation, especially by members of the MYB and AP2/EREBP families (Lee and Suh, 2015a). In Arabidopsis, WAX INDUCER1/SHINE1, which belongs to the

[1] These authors contributed equally to this work.
[2] Address correspondence to shiyoulu@hubu.edu.cn.
The author responsible for distribution of materials integral to the findings presented in this article in accordance with the policy described in the Instructions for Authors (www.plantcell.org) is: Shiyou Lü (shiyoulu@hubu.edu.cn).
www.plantcell.org/cgi/doi/10.1105/tpc.19.00233

AP2/EREBP-type transcription factor (TF) family, and its homologs SHN2 and SHN3, activates cuticular wax synthesis, improving plant drought tolerance (Aharoni et al., 2004; Broun et al., 2004). Recently, *WRINKLED4* (*WRI4*, also a subfamily of AP2/EREBP TF) was reported to be involved in direct activation of genes in the wax synthesis pathway (Park et al., 2016). *DEWAX*, another AP2/ERF TF, negatively regulates wax production in Arabidopsis (Go et al., 2014). Besides AP2/EREBP families, cuticular wax biosynthesis is also regulated by MYB TFs, such as *MYB16*, *MYB30*, *MYB96*, *MYB94*, and *MYB106* (Raffaele et al., 2008; Seo et al., 2011; Oshima et al., 2013; Lee and Suh, 2015b). The transcriptional regulation of wax metabolism by *MYB96* and *MYB30* was also found to participate in plant tolerance to abiotic and biotic stresses, respectively (Raffaele et al., 2008; Seo et al., 2011). Based on the above findings, it is clear that even though many TFs and their targets in wax synthesis have been identified, a more complete understanding of the transcriptional network regulating cuticular wax biosynthesis needs to be addressed (Lee and Suh, 2015a).

Apart from transcriptional regulation, cuticular wax biosynthesis is also regulated at the posttranscriptional level by small RNAs (sRNAs; Hooker et al. 2007; Lam et al. 2012, 2015). *CER7* encodes an exoribonuclease, a core subunit of the RNA-processing/degrading exosome complex, which was first reported to regulate the waxes synthesis on the developing stems of Arabidopsis (Hooker et al. 2007). Through identifying the *cer7* suppressor mutants, Lam et al. (2012) speculated that CER7-mediated exosomal degradation alters the levels of sRNA species, which in turn controls *CER3* expression by gene silencing at the posttranscriptional level. Indeed, the authors further demonstrated that trans-acting small interfering RNAs (tasiRNAs), one type of plant sRNAs, directly control *CER3* expression levels and regulate stem wax deposition (Lam et al. 2015). In addition to tasiRNAs, another type of sRNAs, micro RNAs (miRNAs), plays important roles in gene expression regulatory networks, and affects diverse aspects of plant growth and development at the posttranscriptional level (Borges and Martienssen, 2015). miR156 is one of the few miRNAs that is highly conserved within the plant kingdom (Chuck et al., 2007; Wang et al., 2009, 2011; Wu et al., 2009). miR156 targets members of the plant-specific *SQUAMOSA PROMOTER BINDING PROTEIN LIKE* (*SPL*) transcription factor gene family (Klein et al., 1996; Guo et al., 2008). In Arabidopsis, 10 *SPL* genes have miR156 binding sites either in the coding region or the 3′-untranslated region. They can be further classified into four taxonomic subgroups: *SPL3*/*SPL4*/*SPL5*, *SPL9*/*SPL15*, *SPL2*/*SPL10*/*SPL11*, and *SPL6*/*SPL13* (Cardon et al., 1999; Wu and Poethig, 2006; Gandikota et al., 2007). The miR156-SPL9 module has been found to be involved in multiple biological processes, including phase transition, root and leaf development, and flowering as well as stress responses (Wu and Poethig, 2006; Wang et al., 2009; Gou et al., 2011; Cui et al., 2014; Rubio-Somoza et al., 2014; Yu et al., 2015a). Specifically, the miR156-SPL9 module is reported to regulate secondary metabolism. For example, SPL9 interacts with PRODUCTION OF ANTHOCYANIN PIGMENT1 (PAP1) and decreases anthocyanin biosynthesis through directly regulating *DIHYDROFLAVONOL 4-REDUCTASE* (*DFR*) expression (Gou et al., 2011). Furthermore, Yu et al. (2015b) demonstrated that SPL9 directly binds to the *Terpene Synthase21* (*TPS21*) gene promoter and activates its expression to regulate sesquiterpene production in Arabidopsis and Patchouli (*Pogostemon cablin*). To date, however, whether miR156 or SPLs are involved in wax synthesis is not known.

A previous study reported that DEWAX is a negative regulator of wax accumulation in the dark (Go et al., 2014). However, optimization of the daily light/dark responses would require an additional positive regulator in the light. In this paper, we have shown that SPL9 acts as a positive light-induced regulator of wax synthesis. Our research demonstrates that SPL9 controls *CER1* expression, a rate limiting step in wax alkane synthesis. This is achieved by directly binding to GTAC motifs in the *CER1* promoter. Our data also indicate that SPL9 and DEWAX act antagonistically to control *CER1* expression via direct protein–protein interaction. The sophisticated combinatorial regulation exerted by the SPL9-DEWAX loop constitutes a key molecular mechanism mediating the light-dark on-off switch controlling wax synthesis.

RESULTS

The miR156-SPL9 Module Regulates Wax Synthesis

Alkanes are the major components of cuticular wax, and previous studies have shown that the alkane synthesizing gene *CER1* is expressed in a diurnal cycle (Go et al., 2014). To identify factors responsible for light-regulated wax synthesis, we performed a yeast one-hybrid screen with *CER1* promoter DNA with a prey library composed of ~1500 transcription factor cDNAs of Arabidopsis (Mitsuda et al., 2010). Interestingly, this screen identified a positive clone encoding SPL9. Using a full-length cDNA of *SPL9* inserted into a pGADT7 plasmid, we demonstrated that SPL9 interacted with the *CER1* promoter in a yeast one-hybrid assay via the expression of the *HIS* reporter gene driven by the *CER1* promoter (Figure 1A). *SPL9* has been reported to be a miR156 target, and to participate in multiple plant developmental and secondary metabolic regulatory pathways. However, whether miR156 or SPL9 was involved in wax synthesis has not been demonstrated.

We then obtained miR156- or *SPL9*-related genetic materials that were previously used in other studies (Gou et al., 2011), including *Pro35S:MIR156*, *Pro35S:MIM156*, *ProSPL9:rSPL9*, *spl9-4 spl15-1*. *Pro35S:MIR156* is a transgenic line overproducing miR156, whereas *Pro35S:MIM156* is a transgenic line in which miR156 activity is reduced via target mimicry (Franco-Zorrilla et al., 2007). *Pro35S:MIM156* was used because miR156 is generated from eight separate loci in the Arabidopsis genome and it is difficult to obtain a complete knockout allele of miR156. *ProSPL9:rSPL9* and *spl9-4 spl15-1* were used as SPL9 gain-of-function and loss-of-function lines, respectively. *ProSPL9:rSPL9* expresses a miR156-resistant SPL9 transcript; therefore, *SPL9* was overexpressed. The *spl9-4 spl15-1* double mutant was first chosen for phenotype analysis because SPL15 is the closest paralog of SPL9. As in previous studies, the SPL genes showed a high degree of functional redundancy in development, and single mutants were phenotypically normal as wild-type plants (Wang et al., 2008; Wu et al., 2009). We observed glossy green (*Pro35S:MIR156* and *spl9-4 spl15-1*) or glaucous white (*Pro35S:MIM156*

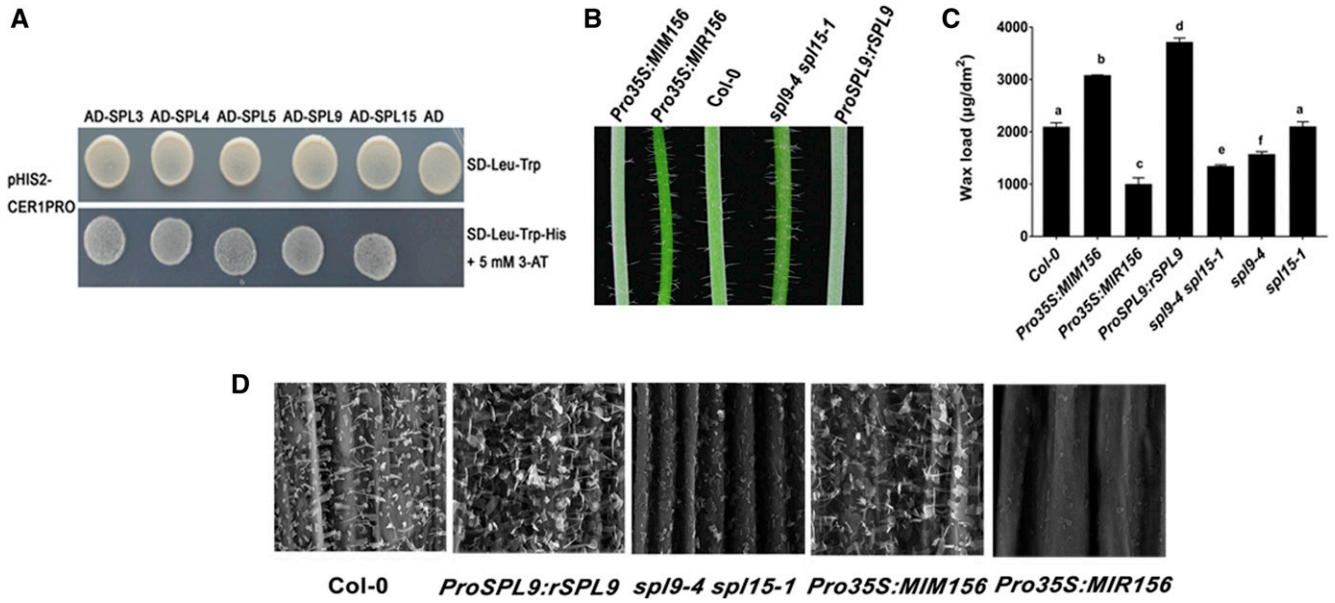

Figure 1. miR156-SPL9 Module Regulates Wax Synthesis.

(A) Yeast one-hybrid assay to dissect the binding of SPLs to *CER1* promoter DNA. For yeast one-hybrid experiment, *CER1* promoter DNA region was fused to the *HIS3* (auxotrophic marker) reporter gene in *pHIS2* plasmid and tested for AD-SPLs binding. Empty pGADT7 vector was used as negative control.
(B) Glossy green and white waxy phenotypes of 6-week-old inflorescence stems of *Pro35S:MIR156*, *Pro35S:MIM156*, and *SPL9* related lines compared with the wild type (Col-0). *Pro35S:MIR156* and *Pro35S:MIM156* are transgenic lines overexpressing miR156 and its artificial miRNA target mimic construct, respectively. *ProSPL9:rSPL9* and *spl9-4 spl15-1* represent SPL9 gain-of-function and loss-of-function plants, respectively.
(C) Cuticular wax amounts of inflorescence stems from 6-week-old wild-type, *Pro35S:MIR156*, *Pro35S:MIM156*, and *SPL9* related Arabidopsis lines, which were grown under long-day conditions (16 h of light/8 h of dark). Cuticular waxes were extracted with hexane and analyzed by GC-FID. Wax coverage is expressed as wax amounts per stem surface area ($\mu g.dm^{-2}$). Error bars indicate means from four replicate experiments, and their SD are shown. The significant differences between samples labeled with different lowercase letters were determined using ANOVA with a post hoc Tukey Honestly Significant Difference test.
(D) SEM images of epicuticular wax crystals on inflorescence stems of 6-week-old wild-type, *Pro35S:MIR156*, *Pro35S:MIM156,* and *SPL9* related Arabidopsis lines. Bars = 5 μm.

and *ProSPL9:rSPL9*) phenotypes in the stems, respectively (Figure 1B).

Consistent with this observation, chemical analysis of wax revealed that total wax loads were increased by ~50% and 70% on *Pro35S:MIM156* and *ProSPL9:rSPL9* stems, respectively, relative to the wild type. By contrast, a substantial decrease in total wax amount was observed on stems of *Pro35S:MIR156* (~47% of wild type, $P < 0.01$) and *spl9-4 spl15-1* (~63% of wild type, $P < 0.01$), relative to the wild type, with *Pro35S:MIR156* displaying the least severe wax defect (Figure 1C).

Using scanning electron microscopy (SEM), we examined the deposition of epicuticular wax crystals on the stem surface of these lines. Relative to wild type, we observed significantly fewer epicuticular wax crystals on the *Pro35S:MIR156* and *spl9-4 spl15-1* stems, and a significantly higher density of epicuticular wax crystals on the *Pro35S:MIM156* and *ProSPL9:rSPL9* stems (Figure 1D). Together, these results indicated that the miR156-SPL9 module has a significant effect on the regulation of epidermal wax synthesis.

To elucidate the role of *SPL9* or *SPL15* in wax biosynthesis, we examined the stem wax contents of the *spl9-4* or *spl15-1* mutant. The total wax loads on *spl9-4* stems were much lower than those in the wild type, whereas *spl15-1* exhibit similar wax accumulation as the wild type (Figure 1C). Furthermore, the wax content of *spl9-4* was significantly higher than that of the *spl9-4 spl15-1* double mutant (Figure 1C), whereas the *Pro35S:MIR156* overexpression transgenic line exhibited the lowest wax content. These data suggest that the production of wax is apparently coordinately regulated by multiple SPLs, with a major contribution of SPL9. Consistent with this idea, several other SPLs including SPL3, SPL4, SPL5, and SPL15 also could bind the *CER1* promoter in yeast one-hybrid assays (Figure 1A). In the following research, we focused our analysis on SPL9. We found that essentially all individual wax constituents were increased in *Pro35S:MIM156* and *ProSPL9:rSPL9* stems relative to the wild type. Particularly, there was a prominent increase in the amounts of the C29 alkanes and C29 ketones in both *Pro35S:MIM156* and *ProSPL9:rSPL9*. Conversely, almost all wax constituents were reduced in *Pro35S:MIR156* and *spl9-4* stems, especially the C29 alkanes and C29 ketones (Figure 2).

To test whether the miR156-SPL9 module regulates wax synthesis in the leaves, the total cuticular wax amounts and compositions on the surface of leaves of the above lines were determined. The total wax amounts on *Pro35S:MIR156* and *spl9-4* leaves were reduced to ~30% and 60% of the wild-type level, respectively.

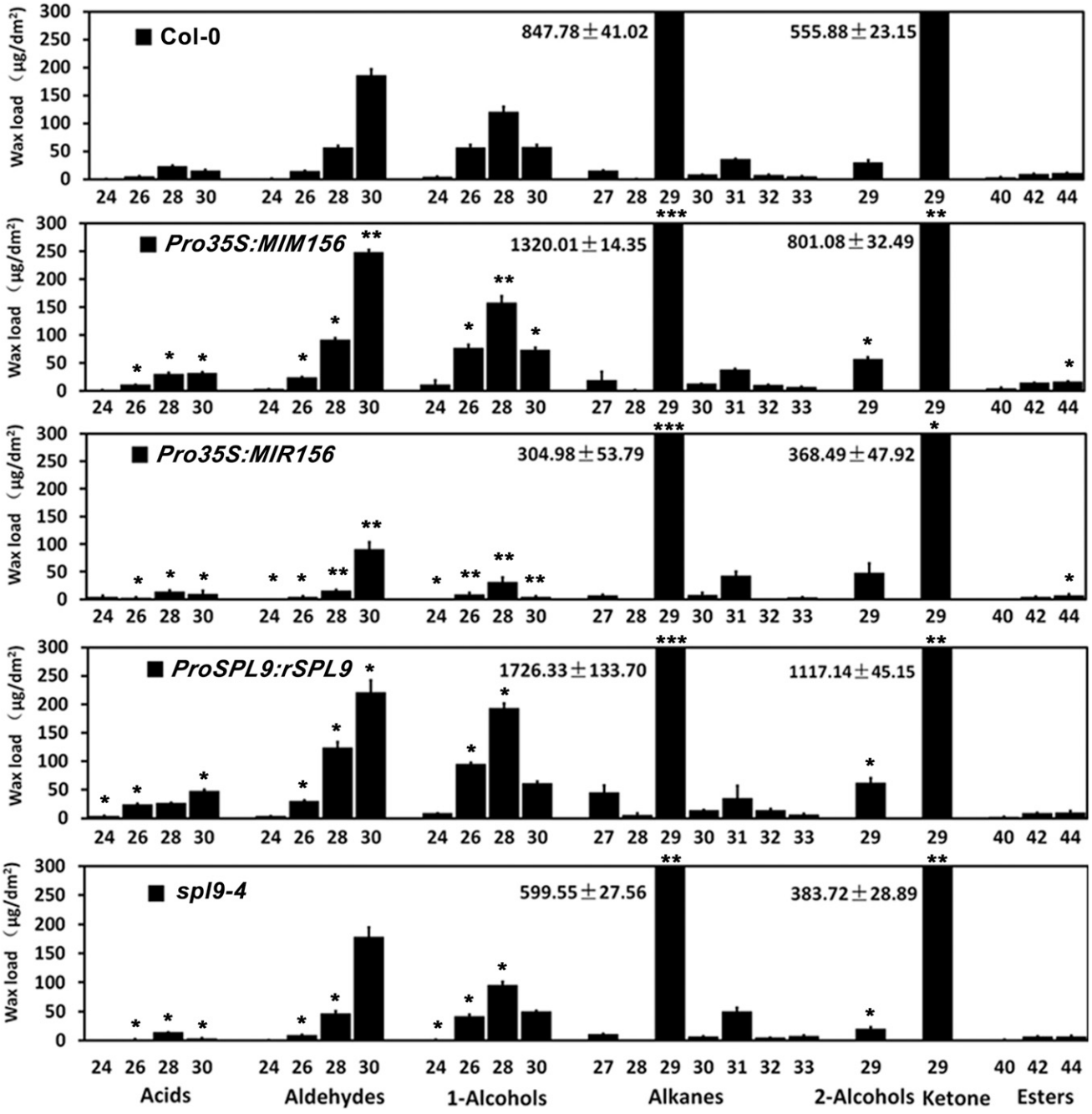

Figure 2. Cuticular Wax Composition of Inflorescence Stems of 6-week-old Wild-Type, *Pro35S:MIR156*, *Pro35S:MIM156*, and *SPL9* Related Arabidopsis Lines.

Wax coverage is expressed as wax amounts per stem surface area ($\mu g.dm^{-2}$). Each wax constituent is designated by carbon chain length and is labeled by chemical class along the *x* axis. Values shown are means $\pm$SD ($n = 4$). The differential significance between transgenic or mutant lines and wild-type plants was determined with Student's *t* test (*P < 0.05; **P < 0.01; ***P < 0.001).

While in *Pro35S:MIM156* and *ProSPL9:rSPL9* leaves, wax loads were increased by ~60% and ~150%, respectively, relative to the wild type (Supplemental Figure 1). The alterations observed in individual wax constituents were most prominent in the C26 and C28 primary alcohols, and the C29, C31, and C33 alkanes (Supplemental Figure 2). Consistent with the higher wax accumulation in *ProSPL9:rSPL9* leaves, epicuticular wax crystals, which are not normally present on wild-type leaves when viewed using SEM, were observed on *ProSPL9:rSPL9* leaf surfaces (Supplemental Figure 3). Overall, these results demonstrate that

SPL9 positively regulates cuticular wax deposition on leaf and stem surfaces.

SPL9 Directly Regulates *CER1* Expression, but Indirectly Regulates *CER4* Expression

To investigate how SPL9 influences wax synthesis at the transcriptional level, RT-qPCR was used to analyze the expression of six representative genes previously associated with wax biosynthesis or transport. Among these genes, *CER1* and *CER3* (also known as *WAX2* or *YRE*) as two components of a multiprotein enzyme complex catalyze the conversion of very long chain acyl-CoAs to very long chain alkanes, which are the most abundant (more than 50% in all organs) wax components in Arabidopsis (Bernard et al., 2012; Lee and Suh, 2015a). *CER4* (also known as *FAR3*) encoding a fatty acyl-CoA reductase converts the VLCFAs into primary alcohols in the alcohol-forming pathway (Rowland et al., 2006). Interestingly, alkane and 1-alcohol amounts were much higher in the stems and leaves of *ProSPL9:rSPL9* than in those of the wild type (Supplemental Tables 1 and 2), indicating both biosynthetic components are simultaneously affected in the two tissues. *CER6* (also known as KCS6, encoding a 3-ketoacyl-CoA synthase) and *CER10* (also known as ECR, encoding an enoyl-CoA reductase) are important for VLCFA elongation (Hooker et al., 2002; Zheng et al. 2005). *CER5* (also known as *ABCG12*, encoding an adenosine triphosphate binding cassette transporter) is responsible for wax transportation to the epidermal surface (Pighin et al., 2004). Among these genes, *CER1* and *CER4* showed significantly enhanced expression (>twofold) in *Pro35S:MIM156* and *ProSPL9:rSPL9*, but decreased expression in *Pro35S:MIR156* and *spl9-4*, in both leaves and stems (Figure 3), which is consistent with the altered compositions of alkanes and primary alcohols we report for these lines. To demonstrate whether SPL9 could modulate *CER1* and *CER4* gene expression in vivo, we constructed the *CER1* and *CER4* promoter luciferase (LUC) reporter plasmids, and performed a transient expression assay in tobacco (*Nicotiana benthamiana*). The results suggested that coexpression of SPL9 protein strongly increased the LUC reporter gene activities driven by the endogenous promoters of *CER1* and *CER4* (Figure 4A). To test whether the differentially expressed *CER1* and *CER4* were direct targets of SPL9, we conducted experiments using transgenic lines expressing the *rSPL9* chimeric protein fused to the glucocorticoid receptor sequence (rSPL9-GR), and exogenous dexamethasone (DEX) exposure to assess nuclear transport and biological activity (Gou et al., 2011). For time-course analysis of gene expression, we chose 0-, 10-, and 30-min and 1-, 3-, 6-, and 12-h treatments of transgenic plants with or without DEX. As *CER1* has been reported to show diurnal rhythmic expression (Go et al., 2014), we calculated the gene expression ratio with and without DEX treatment to exclude other factors possibly affecting *CER1* and *CER4* expression. Interestingly, both *CER1* and *CER4* could be induced by

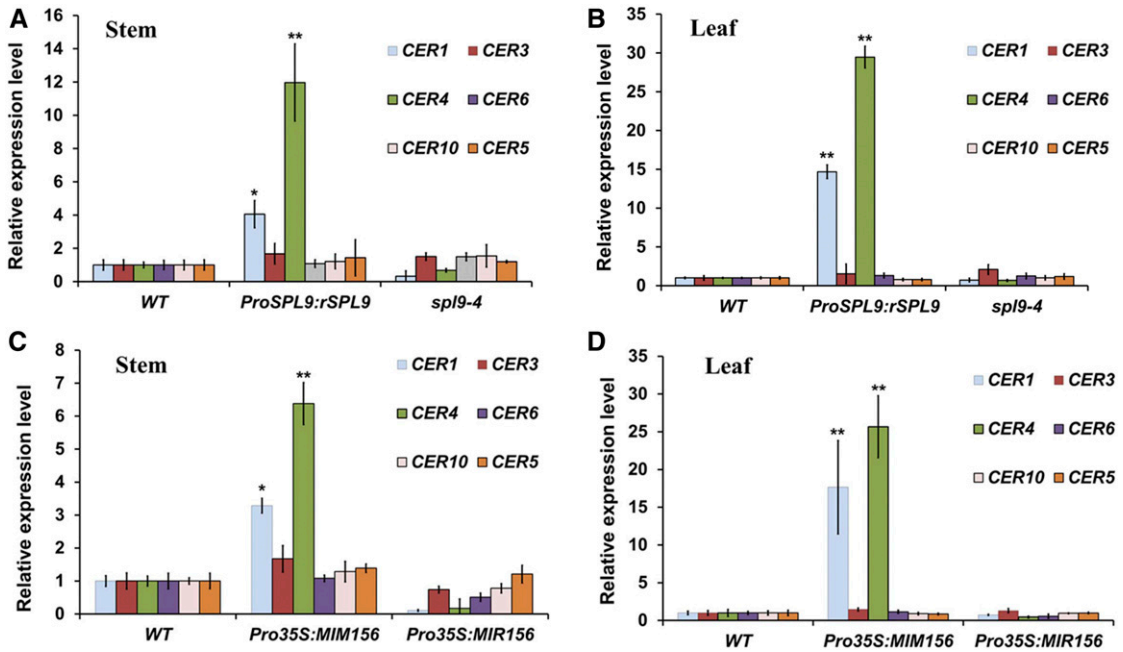

Figure 3. Expression of Wax Synthesis Related Genes in the Stem and Leaf of *Pro35S:MIR156*, *Pro35S:MIM156*, and *SPL9* Related Arabidopsis Lines.

For all the RT-qPCR experiments, the expression level in the wild type (WT) was set as 1. Expression of *PP2A* was used as internal control. Error bars indicate ±SD ($n = 3$). * and **Means differed significantly from WT at $P < 0.05$ and $P < 0.01$, respectively, according to Student's *t* test.

(A) RT-qPCR analysis of wax biosynthetic genes from the stems of 5-week-old wild-type, *ProSPL9:rSPL9*, and *spl9-4* plants.

(B) RT-qPCR analysis of wax biosynthetic genes from the leaves of 3-week-old wild-type, *ProSPL9:rSPL9*, and *spl9-4* plants.

(C) RT-qPCR analysis of wax biosynthetic genes from the stems of 5-week-old wild-type, *Pro35S:MIM156*, and *Pro35S:MIR156* plants.

(D) RT-qPCR analysis of wax biosynthetic genes from the leaves of 3-week-old wild-type, *Pro35S:MIM156*, and *Pro35S:MIR156* plants.

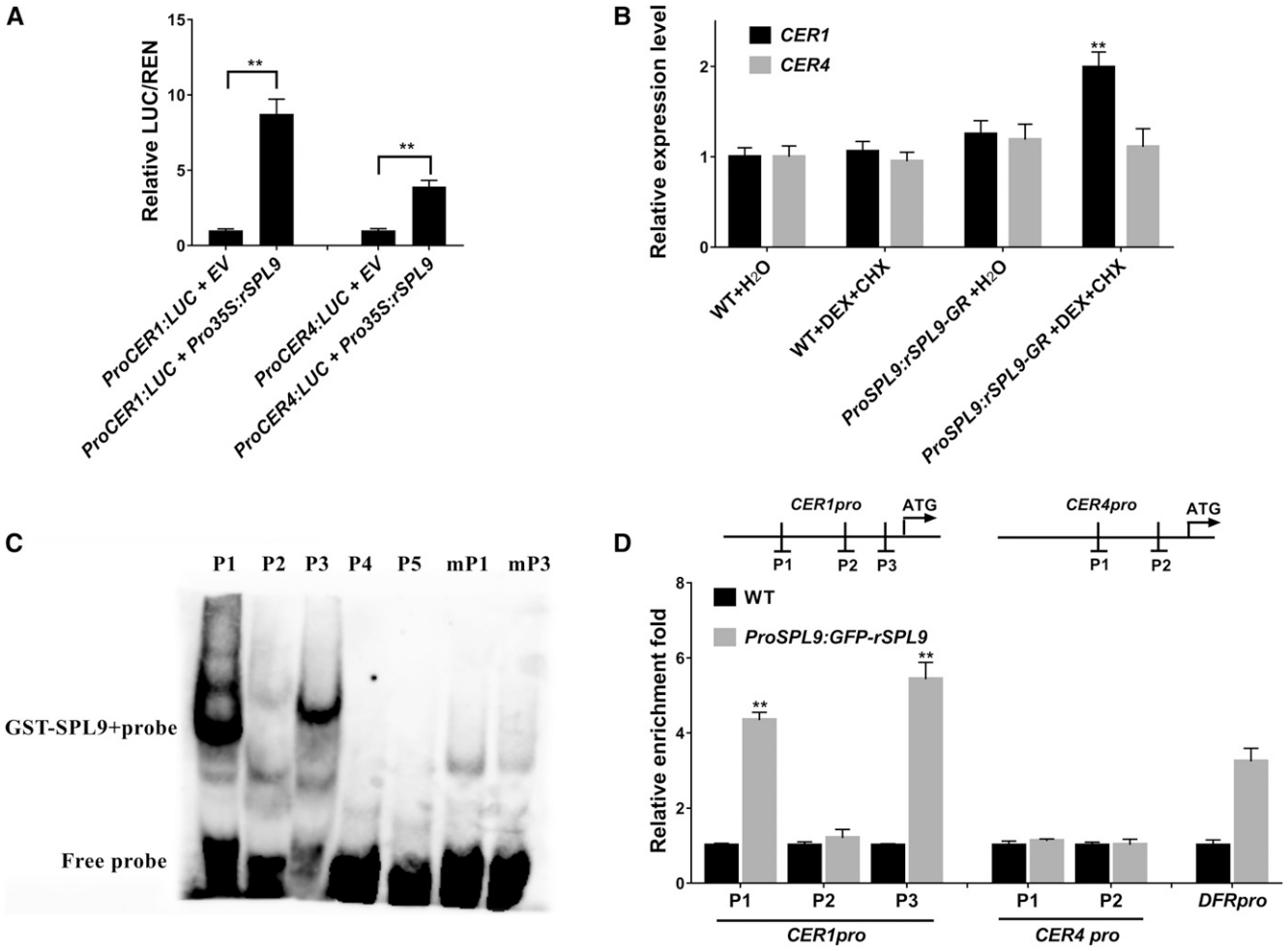

Figure 4. SPL9 Directly Regulates *CER1* Expression, but Indirectly Regulates *CER4* Expression.

(A) SPL9 upregulates *CER1* and *CER4* expression in a transient dual-luciferase reporter system. The coinfiltrations of empty vector (EV) or *Pro35S:rSPL9* with *ProCER1:LUC* or *ProCER4:LUC* reporters were simultaneously expressed in *N. benthamiana* leaves, and the plants were first incubated in dark for 12 h and then in light for 48 h. The relative luciferase luminescence intensities were quantitated using *Renilla* luciferase (*REN*) for normalization. Asterisks indicate significant differences between the indicated means with $P < 0.01$ by Student's *t* test. Data are presented as the means of three independent assays. Error bars represent ±SD ($n = 3$).

(B) Induction of expression of *CER1* and *CER4* in *ProSPL9:rSPL9-GR* plants. Seven-day-old, long day–grown seedlings were treated with either water or DEX and CHX. Seedlings were harvested 6 h after treatment. Expression was normalized relative to that of *PP2A*. Each column represents the mean of three independent assays, each based on over 20 seedlings. Errors bars indicate ±SD (**$P < 0.01$, Student's *t* test). WT, wild type.

(C) EMSAs to test binding of SPL9 to the putative GTAC motifs in the *CER1* (P1-P3) and *CER4* (P4 and P5) promoters, respectively. The GTAC motifs in P1 and P3 were mutated to AAAA in mP1 and mP3 to test the sequence specificity.

(D) ChIP-qPCR confirmed direct binding of SPL9 in the *CER1* promoter. Diagram depicts the putative promoters of *CER1* and *CER4*. PCR amplicons indicated as P1-P3 for the *CER1* promoter and P1/P2 for the *CER4* promoter were used for ChIP-qPCR. Chromatin from 3-week-old Arabidopsis seedlings expressing *ProSPL9:GFP-rSPL9* (Gou et al., 2011) was extracted using anti-GFP antibodies. Wild-type seedlings were used as negative control. qPCR was used to quantify enrichment of SPL9 to promoter regions. SPL9 DNA binding ratio (as revealed by GFP enrichment in ChIP experiments) to the promoter regions was assayed. *DFR* promoter was used as a positive control. Each column represents the mean of three biological repeats. Error bars denote ±SD (**$P < 0.01$, Student's *t* test).

DEX treatment, but the induction times showed large differences. *CER1* could be induced within 10 min and lasted 12 h. However, *CER4* was not induced until 6 h of DEX treatment (Supplemental Figure 4). This result indicates that *CER1* expression can be rapidly induced by sudden changes of SPL9 activity. Moreover, *CER1*, but not *CER4* gene expression, could be enhanced by SPL9 with exogenous exposure to cycloheximide (CHX) and DEX (Figure 4B), raising the possibility that induction of *CER4* expression by SPL9 requires synthesis of additional downstream factors.

SPL9 is known to preferentially recognize DNA motifs with the GTAC sequence (Yamasaki et al., 2009). We identified three and

two typical SPL9 binding sites (GTAC) in the *CER1* and *CER4* promoters, respectively. To test whether SPL9 directly binds to these sequences, we conducted electrophoretic mobility shift assays (EMSAs). For these experiments, complementary oligonucleotides spanning the corresponding GTAC and flanking regions from the *CER1* promoter (P1–P3) and the *CER4* promoter (P4 and P5) were synthesized and labeled with biotin. As shown in Figure 4C, the recombinant GST-SPL9 protein caused a mobility shift of the two probes P1 and P3 in the *CER1* promoter (Figure 4C). However, the P2 probe in the *CER1* promoter and P4 and P5 probes in the *CER4* promoter showed no mobility shift. Furthermore, the probes mP1 and mP3, in which the GTAC motif had been removed by mutations, did not show any shifted band when incubated with GST-SPL9 (Figure 4C), indicating that SPL9 bound specifically to GTAC motifs. To further determine whether SPL9 directly associates with *CER1* promoter in vivo, a chromatin immunoprecipitation (ChIP) assay was performed using transgenic *ProSPL9:GFP-rSPL9* lines (Gou et al., 2011). After the protein–DNA complexes were immunoprecipitated by anti–GFP antibody, the DNA fragments were quantified by qPCR. The promoter region of *DFR* (a gene known to be a direct SPL9 target, Gou et al., 2011) was amplified as a positive control, and the promoter of *ACT2* was amplified as a negative control. Similar to the *DFR* positive control, the P1 and P3 regions of the *CER1* promoter, which include the GTAC motif, were enriched in *ProSPL9:GFP-rSPL9* when compared with the wild type (Figure 4D), consistent with the EMSA results. By contrast, there was no obvious enrichment for regions P2 in *CER1* and P1 and P2 in *CER4* promoters. These results confirmed that *CER1* was a direct target of SPL9 (Figure 4D). Therefore, we suggest that SPL9-mediated direct regulation of *CER1* and indirect regulation of *CER4* expression represents a major regulatory pathway controlling epidermal wax biosynthesis.

CER1 and CER4 are Independently Responsible for SPL9 Regulated Wax Synthesis

Although we have observed that both *CER1* and *CER4* are differentially expressed in miR156-SPL9 related mutants, whether changes in the expression of these genes is responsible for the altered wax phenotype is unknown. To shed light on this, we crossed the loss of function mutants *cer1-2* and *cer4-4* to *ProSPL9:rSPL9* and *Pro35S:MIM156*, respectively, to create the genetic lines *ProSPL9:rSPL9 cer1-2*, *ProSPL9:rSPL9 cer4-4*, *Pro35S:MIM156 cer1-2*, and *Pro35S:MIM156 cer4-4*. As an initial observation, all of these lines exhibited a glossy phenotype comparable with *cer1-2* and *cer4-4* (Supplemental Figure 5). Next, we performed SEM analysis to observe the distributions of epicuticular wax crystals on the stem surface of these lines. Surprisingly, the stem surfaces of all these lines exhibited a much higher density of wax crystals than either *cer1-2* or *cer4-4*, with especially higher crystal density on *ProSPL9:rSPL9 cer1-2* and *ProSPL9:rSPL9 cer4-4* (Figure 5A). To explore the basis for this, we examined the stem wax amounts and wax chemical compositions of these lines using gas chromatography with flame ionization detection (GC-FID). Interestingly, *Pro35S:MIM156 cer1-2*, *Pro35S:MIM156 cer4-4*, *ProSPL9:rSPL9 cer1-2*, and *ProSPL9:rSPL9 cer4-4* showed significantly higher wax accumulation compared with the single *cer1-2* or *cer4-4* mutants, with the accumulation being higher on *ProSPL9:rSPL9 cer1-2* and *ProSPL9:rSPL9 cer4-4* than on *Pro35S:MIM156 cer1-2* and *Pro35S:MIM156 cer4-4* (Figure 5B). When the wax chemical compositions were considered, it was notable that in *ProSPL9:rSPL9 cer1-2* or *Pro35S:MIM156 cer1-2*, the synthesis of primary alcohols was greatly increased compared with the *cer1-2* single mutant (Supplemental Table 1). By comparison, in *ProSPL9:rSPL9 cer4-4* and *Pro35S:MIM156 cer4-4*, the total alkane content was much higher than in *cer4-4* (Supplemental Table 1). Interestingly, although the total wax loads in the stem of *Pro35S:MIM156 cer4-4* and *ProSPL9:rSPL9 cer4-4* lines were higher than in the wild-type plants, these two lines still display a glossy phenotype. Moreover, the data obtained for leaves was similar as in stems, in that *ProSPL9:rSPL9* and *Pro35S:MIM156* exhibited increased wax amounts in the *cer1-2* and *cer4-4* background, with specific upregulation of the primary alcohols or alkanes, respectively (Supplemental Figure 6; Supplemental Table 2). These results indicate that independent regulation of *CER1* and *CER4* by SPL9 are involved in the regulation of wax synthesis. Based on this, we constructed a *cer1-2 cer4-4* double mutant, and *ProSPL9:rSPL9 cer1-2 cer4-4* genetic line, and examined their wax phenotypes. Consistent with our hypothesis, the wax amount in *ProSPL9:rSPL9 cer1-2 cer4-4* was the same as in *cer1-2 cer4-4* (Figure 5C).

SPL9 Specifically Interacts with DEWAX In Vitro and In Vivo

To investigate mechanisms by which the SPL9-dependent signaling cascade regulates wax synthesis, we performed a yeast two-hybrid experiment using SPL9 as the bait against a battery of genes, which have been reported to regulate wax synthesis in Arabidopsis. These genes included positive regulators *WIN1*, *SHN3*, *MYB16*, and *MYB96* and a negative regulator *DEWAX*. SPL9 interacted specifically with DEWAX (Figure 6A). We next examined if DEWAX interact with other SPLs using yeast two-hybrid assays, and the results showed that DEWAX did not interact with SPL3, SPL4, SPL5, or SPL15 (Figure 6B), suggesting that DEWAX interacted specifically with SPL9. Furthermore, we mapped the domain of SPL9 required for the interaction with DEWAX. Y2H assays showed that the SPL9 N-terminal (1–160 amino acids), containing the DNA binding domain, bound to the DEWAX N-terminal (1–100 amino acids) but not to the DEWAX C-terminal (101–201 amino acids) containing the DNA binding domain (Supplemental Figure 7).

Furthermore, the SPL9-DEWAX physical interaction was confirmed by in vitro pull-down assay using recombinant proteins purified from *E. coli*. GST-DEWAX was precipitated with 6xHiS-SPL9, but not with the control alone using Ni-NTA agarose. Similarly, 6xHis-SPL9 was precipitated with GST-DEWAX but not GST alone using anti-GST-beads (Figure 6C). To confirm the SPL9-DEWAX interaction in vivo, we performed bimolecular fluorescence complementation (BiFC) assays with *N. benthamiana* epidermal leaf cells transiently coexpressing *nYFP-DEWAX* and *rSPL9-cYFP*. Strong yellow fluorescent protein

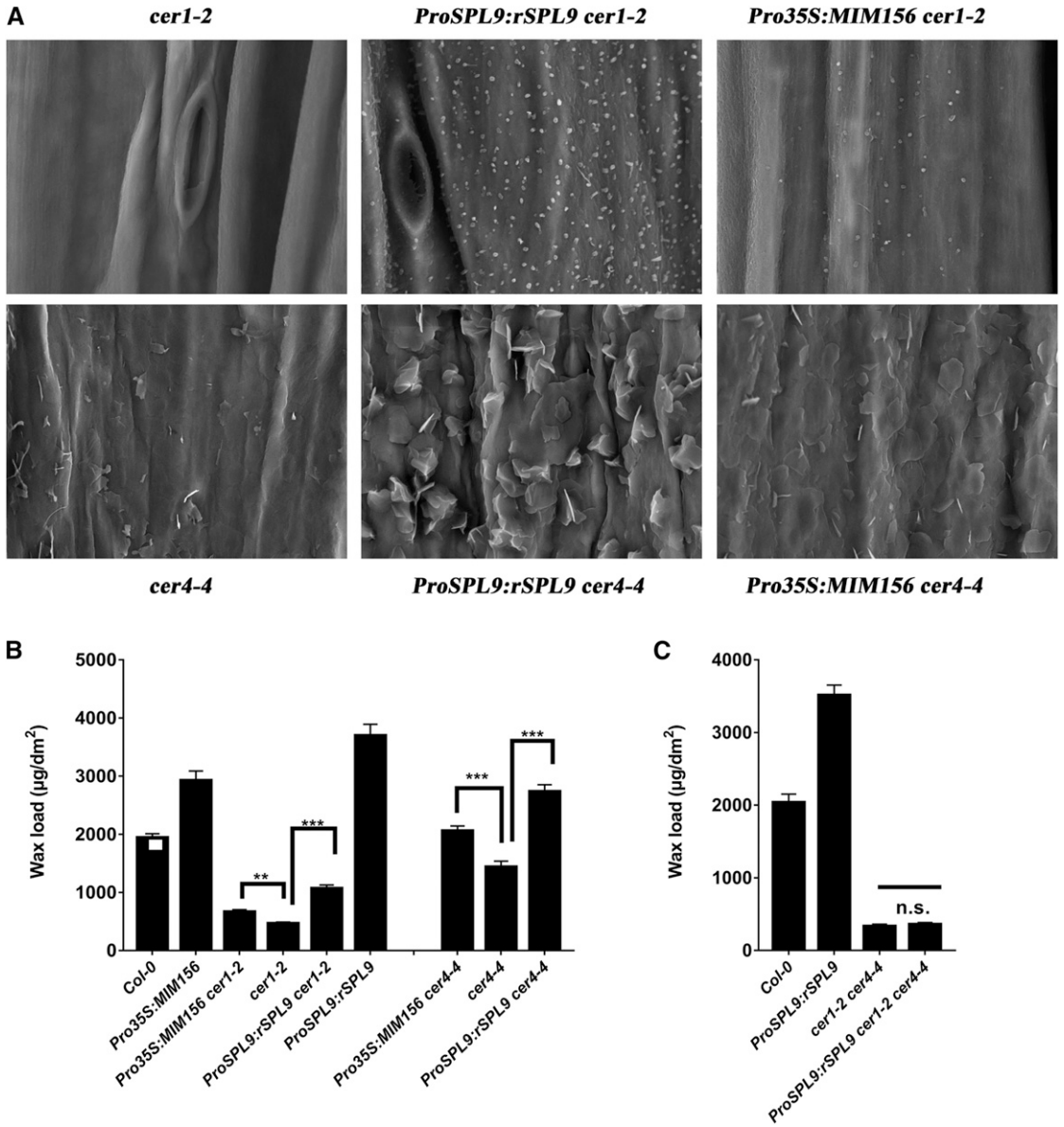

Figure 5. *CER1* and *CER4* Are Independently Responsible for SPL9 Regulated Wax Synthesis.

(A) SEM images of epicuticular wax crystals on inflorescence stems of 6-week-old Arabidopsis crossing lines between *35S:rSPL9* or *35S:MIM156* and *cer1-2* or *cer4-4*. Bars = 5 μm.

(B) Cuticular wax amounts of inflorescence stems from 6-week-old Arabidopsis crossing lines between *35S:rSPL9* or *35S:MIM156* and *cer1-2* or *cer4-4* grown in long-day conditions. Cuticular waxes were extracted with hexane and analyzed by GC-FID. Wax coverage is expressed as wax amounts per stem surface area (μg.dm^{-2}). Error bars indicate ±SD (**P < 0.01, ***P < 0.001, Student's *t* test) from four replicate experiments.

(C) Cuticular wax amounts of inflorescence stems from 6-week-old wild-type, *cer1-2 cer4-4*, and *ProSPL9:rSPL9 cer1-2 cer4-4* mutants. Cuticular waxes were extracted with hexane and analyzed by GC-FID. Wax coverage is expressed as wax amounts per stem surface area (μg.dm^{-2}). Error bars indicate ±SD from four replicate experiments; n.s., no significance by Student's *t* test.

(YFP) fluorescence was observed in the nucleus of cells coexpressing *nYFP-DEWAX* and *rSPL9-cYFP*, but not in those coexpressing *nYFP* and *rSPL9-cYFP* or *nYFP-DEWAX* and *cYFP* (Figure 6D), suggesting a specific interaction of SPL9 with DEWAX. Furthermore, we performed a firefly LUC complementation (BiLC) assay. We fused *rSPL9* to the C-terminal half of LUC (*cLUC-rSPL9*) and *DEWAX* to the N-terminal half of LUC (*DEWAX-nLUC*) and transiently introduced both fusion proteins into tobacco epidermal leaf cells. In the leaves infiltrated with combinations of *Pro35S:nLUC* and *Pro35S:cLUC-rSPL9*, or *Pro35S:cLUC* and *Pro35S:DEWAX-nLUC*, LUC activity was barely detectable. By contrast, leaves that coexpressed *Pro35S:cLUC- rSPL9* and

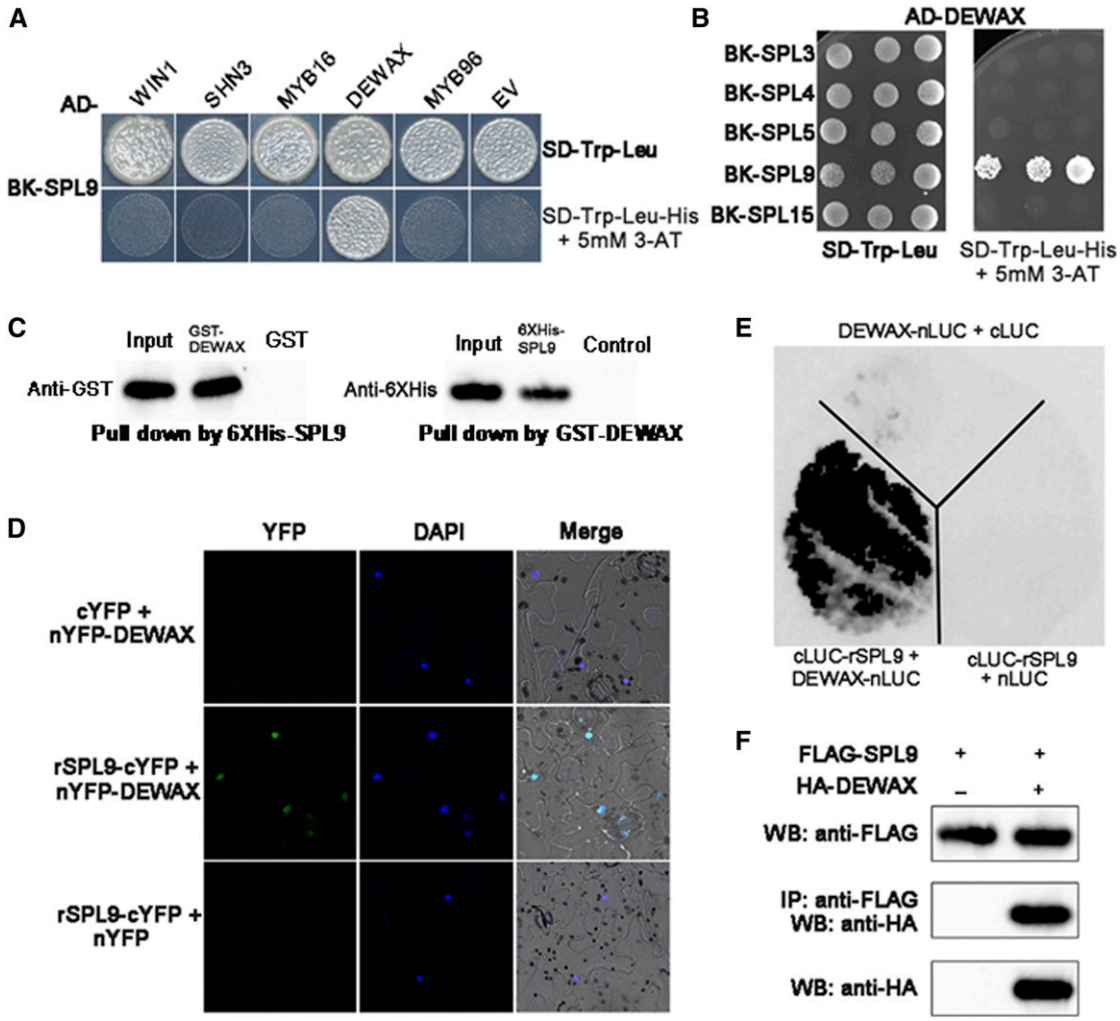

Figure 6. SPL9 Specifically Interacts with DEWAX In Vitro and In Vivo.

(A) Yeast two-hybrid assay shows the specific interaction between SPL9 and DEWAX. SPL9 was in-frame fused to the GAL4 binding domain (BD) in pGBKT7, whereas WIN1, SHN3, MYB16, MYB96, and DEWAX were fused to the GAL4 activation domain (AD) in pGADT7. Transformed yeast cells were grown on SD-Trp-Leu (top). The direct protein interactions were assayed on a SD-Trp-Leu-His plate, supplemented with 5 mM 3-amino-1,2,4,-triazole (3-AT; bottom). The empty pGADT7 were used as negative control.

(B) Interaction analysis of DEWAX with other SPL family proteins (SPL3, SPL4, SPL5, and SPL15) using yeast two-hybrid assays.

(C) An in vitro pull-down assay shows the interaction between SPL9 and DEWAX. 6xHis-SPL9 protein was incubated with immobilized GST or GST-DEWAX protein, and immunoprecipitated fractions were detected by anti-6xHis antibody. Alternatively, GST-DEWAX protein was incubated with immobilized 6xHis-SPL9 or control protein, and immunoprecipitated fractions were detected by anti-GST antibody.

(D) BiFC analysis of the interaction between SPL9 and DEWAX. Blue and green fluorescence represent 4',6-diamidino-2-phenylindole (DAPI) and GFP signals, respectively. The empty nYFP or cYFP vector was used as negative control.

(E) BiLC demonstrates SPL9 interacts with DEWAX in vivo. The leaves of *N. benthamiana* were infiltrated with agrobacteria as indicated. Constructs were combined at a 1:1 ratio. The empty nLUC (N-terminal LUC) or cLUC (C-terminal LUC) vector was used as negative control.

(F) Co-IP assays showing that SPL9 physically associates with DEWAX in vivo. FLAG-SPL9 and HA-DEWAX proteins were transiently expressed in *N. benthamiana*. Protein was immunoprecipitated with anti-FLAG antibody, and the IP fraction was analyzed in a protein blot with anti-HA antibody. The input fraction was analyzed by immunoblotting using either anti-FLAG or anti-HA antibody.

Pro35S:DEWX-nLUC produced a strong LUC signal (Figure 6E). In addition, BiLC experimental results provided evidence that the SPL9 N-terminal DNA binding domain and DEWAX N-terminal domain interacted in vivo (Supplemental Figure 8). Finally, we performed coimmunoprecipitation (Co-IP) experiments to confirm their interaction in vivo. To do this, we coexpressed *FLAG-rSPL9* and *HA-DEWAX* fusion proteins in tobacco leaves. HA-DEWAX coimmunoprecipitated with FLAG-rSPL9 (Figure 6F). Taken together, our data suggest that SPL9 directly binds to DEWAX, both in vitro and in vivo.

DEWAX Inhibits SPL9 Activity in Regulating *CER1* Expression

Although we demonstrated that SPL9 activated wax synthesis, and that SPL9 interacted with the negative regulator DEWAX, it was still uncertain how this interaction was involved in wax synthesis. In transient gene expression assays using the *ProCER1:LUC* construct as a reporter of *Pro35:rSPL9* transcriptional activity, *rSPL9* expression alone resulted in $\alpha\nu$ approximately eightfold activation of the reporter, as anticipated (Figure 7A). Consistent with a previous report (Go et al., 2014), coexpression of *Pro35S:DEWAX* alone inhibited *CER1* expression. Interestingly, coexpression of the SPL9 and the DEWAX proteins led to significantly lower LUC reporter activity, than with SPL9 alone, in a dosage-dependent manner (Figure 7A), suggesting that DEWAX interacts with SPL9 and hampers its transcription activating activity. Additionally, although *CER4* is an indirect target of SPL9, its regulation by the SPL9 and DEWAX interaction appears similar as with *CER1* (Supplemental Figure 9).

Because DEWAX interacts with the SPL9 DNA binding domain (Supplemental Figures 7 and 8), it is possible that this interaction may interfere with SPL9 DNA binding activity. Indeed, in EMSAs, the signal generated by binding of SPL9 to the P1 and P3 probes of the *CER1* promoter was dramatically decreased with increasing DEWAX level, even to a greater extent than observed with exogenous 100× cold competitor probes (Figure 7B), providing evidence that the interaction of the SPL9 DNA binding domain with the *CER1* promoter is attenuated by DEWAX. We next examined how DEWAX regulates SPL9 activity. Intriguingly, BiLC assays showed that expression of *DEWAX* substantially repressed the formation of SPL9 homodimers (Figure 7C), demonstrating that DEWAX possibly inhibits SPL9 protein activity by reducing its DNA binding ability via the formation of nonfunctional heterodimers.

SPL9 Acts Downstream of *DEWAX* in Regulating Epidermal Wax Synthesis

To further explore the antagonistic genetic relationship between *SPL9* and *DEWAX*, we created a series of unique genetic lines by crossing *spl9-4*, *ProSPL9:rSPL9* and *Pro35S:MIM156* with the *DEWAX* loss of function mutant *dewax* or overexpression line *DXOE* and analyzed their wax compositions. As expected, when *DEWAX* was overexpressed in the *ProSPL9:rSPL9* background, the stem wax content of the *DXOE ProSPL9:rSPL9* double mutant was greatly decreased compared with *ProSPL9:rSPL9* (Figure 8A). Similar results were also observed in the *DXOE Pro35S:MIM156* line when compared with the *Pro35S:MIM156* line (Figure 8B). In addition, although the *dewax* knockout mutant showed enhanced wax synthesis compared with the wild type, when *dewax* was placed in the *ProSPL9:rSPL9* or *Pro35S:MIM156* backgrounds, the wax contents of *ProSPL9:rSPL9 dewax* or *Pro35S:MIM156 dewax* lines exhibited no further increases in comparison with *ProSPL9:rSPL9* or *Pro35S:MIM156* (Figures 8A and 8B). More importantly, the double mutant *spl9-4 dewax* displayed a similarly reduced wax content phenotype as that of *spl9-4*, but different from the higher wax content phenotype of *dewax* (Figure 8A). These results lend further evidence that DEWAX suppresses SPL9 protein function. Consistent with the phenotype observed, *CER1* expression *ProSPL9:rSPL9Pro35S:MIM156* was reduced in the *DXOE Pro35S:MIM156* and *DXOE ProSPL9:rSPL9* lines compared with their parent lines *Pro35S:MIM156* or *ProSPL9:rSPL9*, whereas *CER1* expression was similarly reduced in *spl9-4 dewax* and

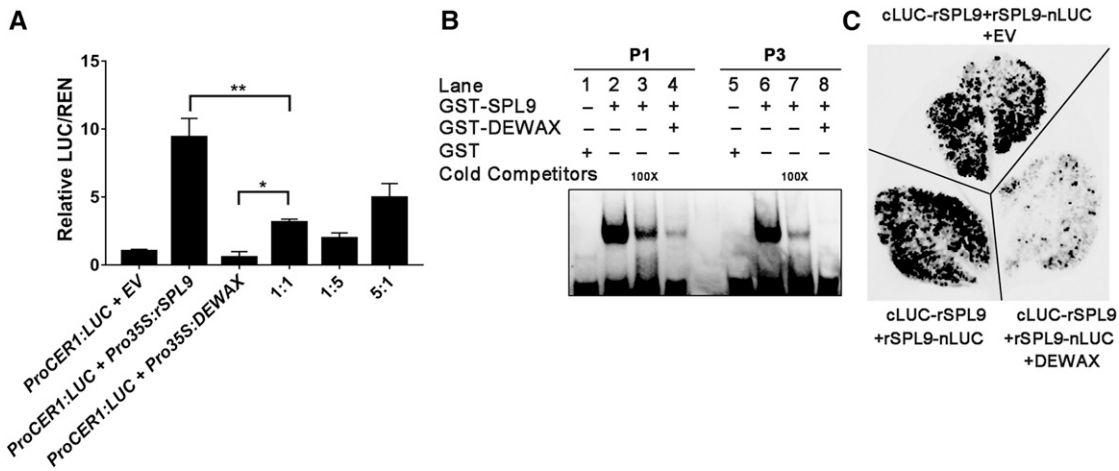

Figure 7. DEWAX Represses DNA Binding Ability of SPL9.

(A) DEWAX represses the SPL9 transcriptional activity on the *CER1* promoter in the transient expression system. *Pro35S:rSPL9* or *Pro35S:DEWAX* alone, or *Pro35S:rSPL9*/*Pro35S:DEWAX* in different ratios with the reporter *ProCER1:LUC* were coinfiltrated and simultaneously expressed in *N. benthamiana* leaves. The relative LUC activity in the coexpressed samples was calculated by normalizing the LUC values against REN. Averages from three biological replicates and their SD are shown. The values were statistically treated using Student's *t* test (*$P < 0.05$, **$P < 0.01$).

(B) EMSAs show that SPL9-DEWAX protein interaction attenuates the DNA binding ability of SPL9 to the GTAC motifs in the promoter region of *CER1*. GST protein was used as negative control. Unlabeled cold competitor probes were used as positive control for attenuated DNA binding.

(C) DEWAX hampers SPL9 homodimer formation in a BiLC experiment. *N. benthamiana* leaves were infiltrated with agrobacteria as indicated.

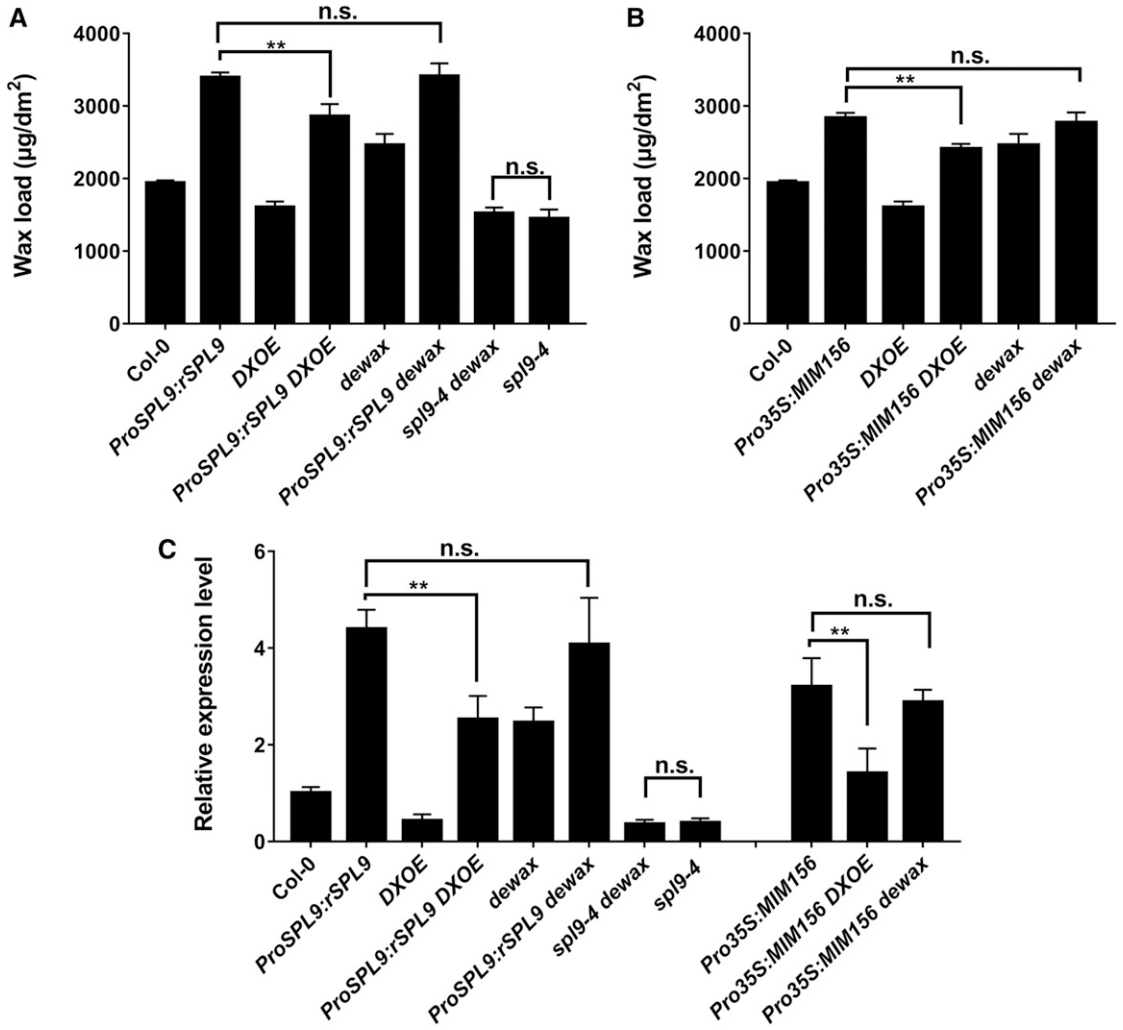

Figure 8. *SPL9* Acts Downstream of *DEWAX* in Wax Synthesis.

(A) Genetic relationship analysis of *SPL9* and *DEWAX* in wax synthesis with double mutant phenotype analysis. Cuticular wax amounts of inflorescence stems from 6-week-old double mutants between *Pro35S:rSPL9*, *spl9-4*, *dewax*, and *DXOE* grown in long-day conditions were examined by GC-FID. Wax coverage is expressed as wax amounts per stem surface area ($\mu g.dm^{-2}$). Error bars indicate ±SD (**P < 0.01, Student's *t* test) from four replicate experiments; n.s. represents no significant difference.

(B) Genetic relationship analysis of miR156 and *DEWAX* in wax synthesis with double mutant phenotype analysis. Cuticular wax amounts of inflorescence stems from 6-week-old double mutants between *Pro35S:MIM156* and *dewax* or *DXOE* grown in long-day conditions were examined by GC-FID. Wax coverage is expressed as wax amounts per stem surface area ($\mu g.dm^{-2}$). Error bars indicate ±SD (**P < 0.01, Student's *t* test) from four replicate experiments; n.s. represents no significant difference.

(C) RT-qPCR analysis of *CER1* expression in the indicated mutants. Expression was normalized relative to that of *PP2A*. Expression level in the wild type (WT) was set as 1. Each column represents the mean of three independent assays, and the error bars indicate ±SD (**P < 0.01, Student's *t* test); n.s. represents no significant difference.

spl9-4 compared with wild-type plants (Figure 8C). These results, combined with the above molecular data, support the idea that *SPL9* acts downstream of *DEWAX* in regulating wax synthesis.

SPL9 and *DEWAX* Expression Are Regulated by Diurnal Cycle And Light/Dark Changes

A previous study has found that *CER1* expression occurs in diurnal patterns and that DEWAX may inhibit its expression in the dark (Go et al., 2014). However, how *CER1* expression is activated in light is unknown. With our findings that SPL9 interacts with DEWAX, and that SPL9 activates *CER1* gene expression, we hypothesized that SPL9-DEWAX may form a regulatory circuit for light/dark-mediated wax synthesis. We analyzed 7 dold wild-type seedlings grown on Murashige and Skoog agar plates in long day (LD) conditions, collected the samples every 3 h in one diurnal cycle, and then examined the gene expression of *CER1*, *SPL9*, and *DEWAX*. In accordance with previous findings, *CER1* expression

was higher in the day and lower in the night. Interestingly, *SPL9* also showed a diurnal expression pattern, with highest expression in the light at Zeitgeber time (ZT)10, similar to *CER1*, suggesting that *SPL9* may be involved in the regulation of diurnal *CER1* expression (Figure 9A). Furthermore, to explore whether *SPL9* diurnal expression was regulated by miR156 at the posttranscriptional level, we examined the expression of two major *MIR156* primary transcripts of *MIR156A* and *MIR156C* (*pri-MIR156A* and *pri-MIR156C*) and mature miR156 at four time points (ZT4, 10, 16, and 22) by RT-qPCR. The results suggested that the expression of *pri-MIR156A* and *pri-MIR156C* were decreased in the day and increased during the night, opposite to *CER1* and *SPL9* expression. Furthermore, the expression of mature miR156 was similar to that of its precursors, consistent with its speculated role in the negative regulation of *SPL9* (Supplemental Figure 10). Surprisingly, *SPL9* was still expressed diurnally in the miR156-resistant transgenic line *ProSPL9:rSPL9* (Figure 9B). Additionally, in *Pro35S:MIR156* and *Pro35S:MIM156*, the diurnal expression pattern of *SPL9* was similar to the ztwild type, although the oscillation amplitude differed (Figure 9B). These results indicated that diurnal expression of *SPL9* is partially independent of miR156 at the transcriptional level.

In contrast with *CER1* and *SPL9*, *DEWAX* expression oscillated twice a day, once in the day (ZT10) and again in the night (ZT16), consistent with a previous report (Go et al., 2014). Interestingly, *SPL9* also showed highest expression at ZT10 (Figure 9A). Therefore, we assessed the expression of *DEWAX* in *ProSPL9:rSPL9* and *spl9-4*. *DEWAX* expression was significantly elevated in *ProSPL9:rSPL9* and decreased in *spl9-4,* especially at ZT10 (Figure 9C), suggesting that SPL9 was involved in regulating *DEWAX* expression in the day. By searching the *DEWAX* promoter region, we found two potential SPL9 binding sites (GTAC at −1264 to −1261 and −1366 to −1363 bp relative to the ATG start codon, respectively). ChIP-qPCR results showed that the P1 and P2 regions containing GTAC motifs in the *DEWAX* promoter were enriched in *ProSPL9:GFP-rSPL9* as compared with the wild type (Supplemental Figure 11). Consistently, Y1H experiments demonstrated that SPL9 binds the 1.5-kb upstream promoter DNA with these two GTAC motifs, but does not bind the 1.2-kb upstream promoter DNA without these two motifs, supporting the idea that the two sites were required for SPL9 binding. To determine whether SPL9 modulates *DEWAX* expression, we performed transient expression assays with the *DEWAX* promoter LUC reporter in *N. benthamiana*. Coexpression of SPL9 strongly provoked the activity of the LUC reporter gene driven by the 1.5-kb promoter of *DEWAX*. Interestingly, the LUC reporter gene activity driven by the 1.2-kb promoter of *DEWAX* was expressed at a lower level, which is not activated by SPL9 (Supplemental Figure 11). In sum, these results indicate that SPL9 directly binds *DEWAX* promoter DNA and activates its gene expression in vivo. SPL9 and DEWAX may operate in a negative feedback loop important in moderating the light response in wax synthesis.

To test whether the diurnal expression patterns of *SPL9* or *DEWAX* are regulated by the circadian clock, we performed artificially controlled light/dark change experiments. Wild-type plants were grown in long-day conditions for 7 d, and at ZT4 (light) the seedlings were kept in light or transferred to dark condition for 6 h. Both of the seedlings at ZT10 were collected and referred to as light–light and light–dark, respectively. Similarly, seedlings at ZT16 (dark) were held in dark or transferred to light conditions for 6 h. Both seedlings at ZT22 were collected and referred to as dark–dark and dark–light, respectively. As shown in Figure 9D, after the transfer, light treatment increased *SPL9* expression and decreased *DEWAX* expression. By contrast, dark treatment increased *DEWAX* expression and decreased *SPL9* expression. Importantly, the diurnal expression pattern of *SPL9* (higher at ZT10 for light–light compared with dark–dark at ZT22) or *DEWAX* (higher at ZT22 for dark–dark compared with light–light at ZT10) was totally conversed, as *SPL9* showed higher expression at ZT22 (dark–light) than at ZT10 (light–dark) and vice versa for *DEWAX*. The results indicated that the oscillating expression pattern of *SPL9* or *DEWAX* was mainly controlled by light and dark exposure, but not the circadian clock. Furthermore, expression of *pri-MIR156A* and *pri-MIR156C* and mature miR156 during light/dark changes was examined by RT-qPCR. The results suggested that the expressions of *pri-MIR156A*, *pri-MIR156C*, and mature miR156 were inhibited by light and improved by dark treatment (Supplemental Figure 12). Similar to the above diurnal cycle results, when we examined the expression of *SPL9* in *ProSPL9:rSPL9*, *Pro35S:MIR156*, and *Pro35S:MIM156*, the expression alterations still appeared (Figure 9E). These results implied that miR156-independent factor(s) may be involved in regulating *SPL9* expression levels during changes from light to dark, and vice versa.

Finally, to test whether the light and dark changes of *SPL9* or *DEWAX* expression influenced *CER1* expression, we examined *CER1* expression in *ProSPL9:rSPL9*, *spl9-4*, and *dewax*. *CER1* expression still exhibited a strong response to light and dark conditions in these lines (Figure 9F), suggesting that *SPL9* and *DEWAX* play a primary role in regulating the amplitude of light responsiveness of wax synthesis.

Both SPL9 and DEWAX Protein Expression Is Regulated by the Diurnal Cycle

The temporal expression patterns of *SPL* transcripts do not always reflect protein levels and function, as miR156 may regulate *SPL* genes through translational repression. To examine the diurnal expression of SPL9 protein, we took advantage of reporter lines *ProSPL9:SPL9-β-glucuronidase* (*GUS*) and *ProSPL9:rSPL9-GUS* containing miR156-sensitive or miR156-resistant genomic constructs of the gene fused to GUS, respectively. For comparison, we also constructed a transgenic line *ProDEWAX:DEWAX-GUS* to explore impacts of the in vivo protein level of DEWAX. Consistent with the gene expression patterns, GUS staining was higher in the light and lower in the dark in *ProSPL9:SPL9-GUS*. For *ProDEWAX:DEWAX-GUS*, the GUS staining was lower in the light and higher in the dark. *ProSPL9:rSPL9-GUS* still showed higher GUS staining in the light and lower in the dark (Figure 10A), consistent with miR156-independent gene expression alterations (Figure 9B). For the dark-to-light treatment of seedlings at ZT22, we observed higher expression of SPL9 and lower expression of DEWAX protein, in comparison with seedlings at Z22 in the normal growth conditions (Figure 10A). For the light-to-dark treatment seedlings at ZT10, we observed higher expression of the DEWAX and lower expression of the SPL9 protein, compared with the seedlings at Z10 in normal growth conditions. The results further demonstrated that light and

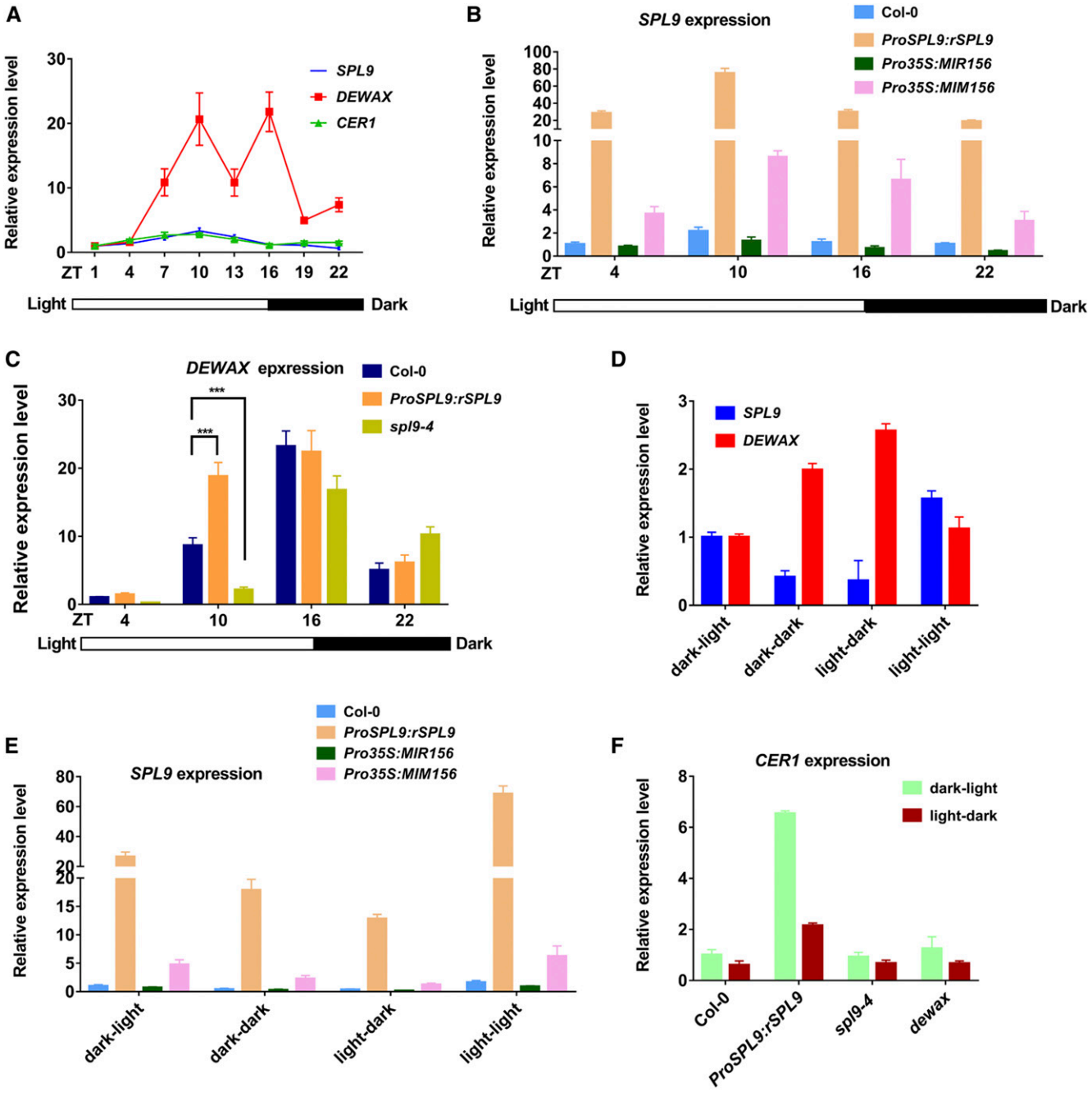

Figure 9. Diurnal Cycles or Light/Dark Changes Affect SPL9 and DEWAX Gene Expression at Multiple Levels.

(A) Diurnal expression of *CER1*, *SPL9*, and *DEWAX*. Gene expression was analyzed in 7-d-old Arabidopsis wild-type seedlings, which were grown under long-day conditions (16 h of light/ 8 h of dark). The light is on at Zeitgeber time 0 (ZT0) and off at ZT16. Total RNA was extracted from at least 20 seedlings (every 3 h from ZT1) and subjected to RT-qPCR analysis. Errors bars indicate ±SD with at least three replicates.

(B) Diurnal expression of *SPL9* is at least partially independent of miR156. Seven-day-old seedlings at four time points (ZT4, ZT10, ZT16, and ZT22) in four different genetic materials (Col-0, *ProSPL9:rSPL9*, *Pro35S:MIR156*, and *Pro35S:MIM156*) were collected, and *SPL9* expression was analyzed by RT-qPCR. Error bars indicate ±SD with at least three replicates.

(C) SPL9 positively regulates *DEWAX* expression in the day. Seven-day-old seedlings at four time points (ZT4, ZT10, ZT16, and ZT22) in Col-0, *ProSPL9:rSPL9*, and *spl9-4* were collected, and *DEWAX* expression was analyzed by RT-qPCR. Errors bars indicate ±SD with at least three replicates. ***$P < 0.001$, Student's *t* test.

(D) Light/dark changes regulate *SPL9* and *DEWAX* expression. For light-dark treatment, at ZT4, 7-d-old seedlings were placed at dark conditions (light-dark) and the controls were maintained at light (light-light). At ZT10, both plants were collected. For dark-light treatment, at ZT16, 7-d-old seedlings were placed at

dark conditions, but not circadian signals, regulate SPL9 and DEWAX protein levels. Moreover, to quantify GUS fusion protein levels, 4-methylumbelliferyl β-D-glucuronide (MUG) assays were performed. The quantification results were consistent with the histochemical staining experiments (Figure 10B). Finally, it should be noted that the expression levels of *DEWAX* in ZT10 and ZT16 were similar, but their protein levels showed significant differences (Figure 10A). This phenomenon prompted us to think that there may be a posttranslational mechanism that regulates DEWAX protein stability. Indeed, when the *ProDEWAX:DEWAX-GUS* seedlings were treated with the 26S proteasome inhibitor MG132, the GUS signals in ZT10 or dark-to-light samples were greatly increased (Figure 10C). The results suggested that light may regulate DEWAX protein level through protein degradation pathways.

SPL9-DEWAX Regulates Diurnal Wax Synthesis

Although we have demonstrated that SPL9-DEWAX modulated diurnal *CER1* expression, it is unknown whether this regulation affects diurnal wax synthesis. To address this question, it would theoretically be necessary to design an experiment to track surface wax accumulation in a diurnal manner (within 24 h). However, this might not be possible or practical. Some experiments by Jenks et al. (1994) with *Sorghum* indicate that measurable wax accumulation is delayed at least 24 h after induction by light. In Arabidopsis, it would likely be even more difficult since there is much less total wax than in *Sorghum*. Thus, we investigated the long-term effects of the length of day or night, or photoperiod, on wax accumulation. First, we examined the expression patterns of *CER1*, *SPL9*, and *DEWAX* under short day (SD; 8/16) conditions. Seven-day-old wild-type seedlings grown on MS-agar plates in SD conditions were collected every 3 h in one diurnal cycle, and the transcript levels were investigated by RT-qPCR. *CER1* and *SPL9* displayed a similar expression pattern as shown in LD conditions, i.e., higher in the day and lower in the night in SD conditions (Figure 11A). However, the expression levels of *CER1* and *SPL9* peaked between ZT4 and ZT7 under SD conditions, which advanced as compared with LD (the highest expression at ZT10). As for *DEWAX*, expression was significantly increased (over 64-fold) at the beginning of the night in SD and still maintained a higher level until light (from ZT10 to ZT22; Figure 11A). The altered expression pattern of *CER1*, *SPL9*, and *DEWAX* motivated us to investigate whether SD conditions change the wax accumulation. Indeed, the short daylength greatly reduced the total wax loads on the stems of wild-type plants (Figure 11B). In LD conditions, the total wax on the stems of wild type was ~2067.97 ± 105.39 μg/dm^2, whereas in SD conditions, it was ~47% lower (~1096.29 ± 28.08 μg/dm^2). We also assessed the stem wax contents of mutant plants in SD conditions. Like in LD, *ProSPL9:rSPL9* and *dewax* in SD conditions contain increased wax loads, whereas *spl9-4* and *DXOE* plants have reduced wax loads compared with wild type (Figure 11B). The daylength also apparently affects the wax accumulation in these mutants since the wax loads in these mutants in SD conditions are far lower than in LD conditions. However, we noticed that the reduction rate in *ProSPL9:rSPL9*, *spl9-4*, and *DXOE* in SD conditions is markedly lower than in wild-type plants (Figure 11C). These results reinforce the idea that SPL9-DEWAX participate in the diurnal or daylength regulated wax accumulation.

Collectively, our results showed that, on one hand, SPL9 and DEWAX protein levels exhibit strong diurnal shifts through transcriptional, posttranscriptional, and/or posttranslational regulation, and on the other hand, SPL9 protein activity was modulated by DEWAX interaction. The two mechanisms may operate together to moderate *CER1* rhythmic gene expression and wax accumulation through the light/dark cycle.

DISCUSSION

Cuticular waxes form the plant's outermost barrier between the plant and its environment, and previous studies show that the plant's cuticle structure and chemical components can change substantially in response to different environmental stimuli (such as temperature, water, pathogen, and phytophagous insect), resulting in a modified cuticle better able to protect the plant (Shepherd and Wynne Griffiths, 2006; Bourdenx et al., 2011; Bernard and Joubès 2013; Lee and Suh, 2015a). And yet, the regulatory mechanisms that determine these precise cuticle responses remain mostly undefined. In this paper, we report a novel mechanism for wax synthesis regulation by the miR156-SPL9 module, expanding knowledge of the environmental regulation of the cuticle to the posttranscriptional level. These and downstream regulatory mechanisms were further described using molecular and genetic approaches, and these results generate key findings that shed light on the role of surface waxes and wax-related genes in the plant environmental response.

Roles of the miR156-SPLs Module in Wax Synthesis Regulation

sRNAs (21 to 24 nucleotide) are noncoding signaling molecules involved in multiple biological pathways (Samad et al., 2017). sRNAs can be classified into two categories including miRNAs

Figure 9. (continued).

light conditions (dark-light) and the controls were maintained at dark (dark-dark). At ZT22, both plants were collected. Total RNAs were extracted from these seedlings collected from the above treatments, and *SPL9* and *DEWAX* expression were analyzed by RT-qPCR. Errors bars indicate ±SD with at least three replicates.

(E) Light/dark changes altered *SPL9* expression at least partially independently of miR156. The treatment processes were as indicated in **(D)**. Seven-day-old seedlings from different genetic materials (Col-0, *ProSPL9:rSPL9*, *Pro35S:MIR156*, and *Pro35S:MIM156*) were collected, and *SPL9* expression was analyzed by RT-qPCR. Error bars indicate ±SD with at least three replicates.

(F) SPL9 only regulates the expression amplitude of *CER1* under light/dark change conditions. *CER1* expression in Col-0, *ProSPL9:rSPL9*, *spl9-4*, and *dewax* is shown. Seven-day-old seedlings during light/dark change conditions were analyzed by RT-qPCR. Error bars indicate ±SD with at least three replicates.

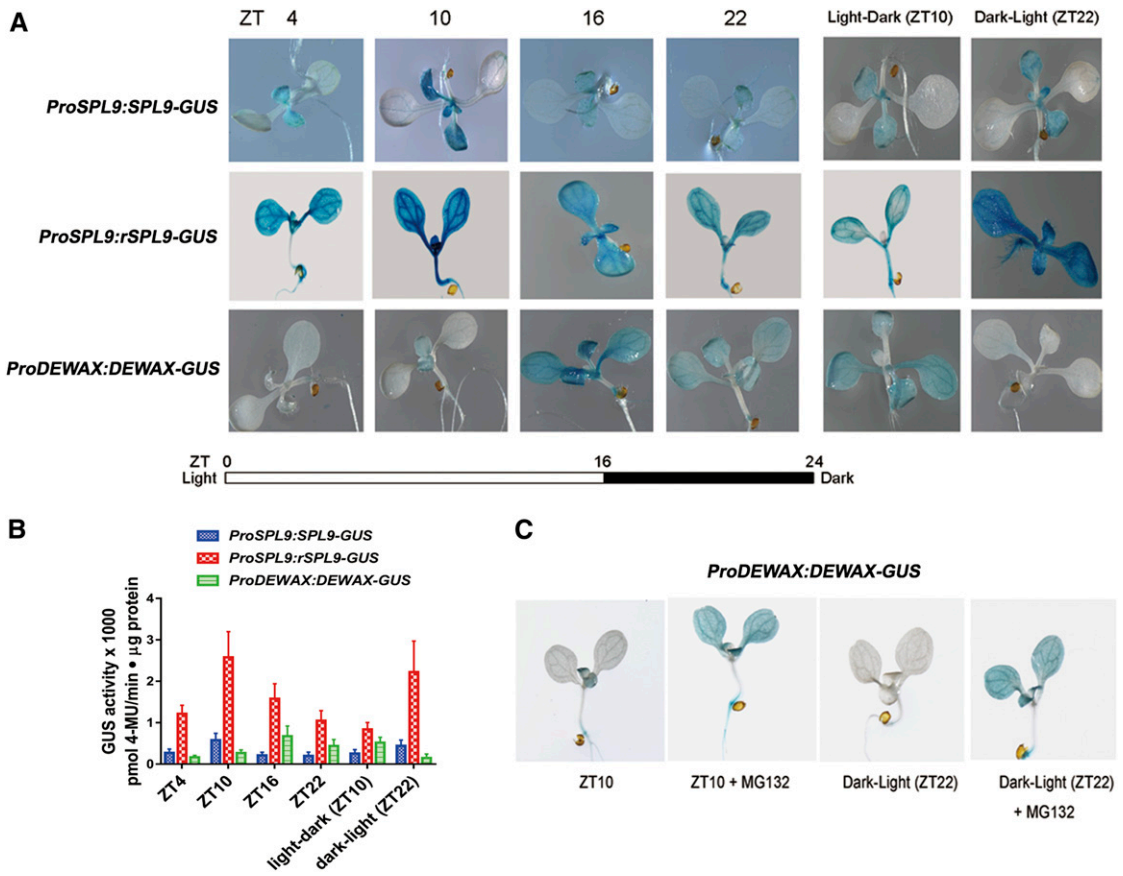

Figure 10. Diurnal Cycles or Light/Dark Changes Affect SPL9 and DEWAX Protein Accumulation.

(A) Diurnal expression of SPL9 and DEWAX protein levels revealed by GUS reporter lines. Histochemical detection of GUS activity driven by the native gene *ProSPL9:SPL9-GUS* or mutated miR156-resistant gene *ProSPL9:rSPL9-GUS* and the native protein *ProDEWAX:DEWAX-GUS* is shown. Seven-day-old seedlings were collected every 6 h from ZT4 in long-day conditions. For light-dark treatment, at ZT4, 7-d-old seedlings were placed at dark conditions and the controls were maintained at light. At ZT10, both plants were collected and GUS activity was stained. For dark-light treatment, at ZT16, 7-d-old seedlings were placed at light conditions and the controls were maintained at dark. At ZT22, both plants were collected and GUS activity was stained. The experiments were repeated three times, and similar results were obtained.

(B) MUG assays for the quantitative analysis of GUS activity in extracts of the samples illustrated in **(A)**. Errors bars indicate ±SD with at least three replicates.

(C) DEWAX protein stability was regulated at the posttranslational level. For MG132 treatment, at ZT4, 7-d-old seedlings were placed on an MS plate with 50 µM MG132 and the controls were maintained on an MS plate. At ZT10, both plants were collected and GUS activity was measured. For dark-light treatment, at ZT16, 7-d-old seedlings were placed on an MS plate with 50 µM MG132 and the controls were maintained on an MS plate. Both plates were placed in light conditions. At ZT22, both seedlings were collected and GUS activity was measured. The experiments were repeated three times, and similar results were obtained.

and small interfering RNAs (siRNAs), based on their differences in the biogenesis and mode of action. miRNAs are processed from a single stranded noncoding RNA precursor that forms a hairpin structure. By contrast, tasiRNAs biogenesis requires an initial process of specific miRNA-mediated cleavage of their TAS RNA precursors through the role of *RNA-DEPENDENT-RNA-POLYMERASE-6* (*RDR6*). The biogenesis of miRNA and tasiRNA also shares the same components, such as HUA ENHANCER1 and ARGONAUTE1 (Borges and Martienssen, 2015). Lam et al. (2015) demonstrated that tasiRNAs directly silence *CER3* expression. In this study, we found that the miR156-SPL9 module directly regulates *CER1* expression. Intriguingly, CER1, CER3/WAX2/YRE, and the cytochrome b5 isoforms constitute a multiprotein enzyme complex in the alkane-forming pathway (Chen et al., 2003; Rowland et al., 2007; Bourdenx et al., 2011; Bernard et al., 2012). Whether there is crosstalk between the two classes of small RNAs (miRNA and tasiRNA) in balancing CER1 and CER3 dosage for their complex formation in wax synthesis is now something to be considered further.

Previous studies have shown that *CER1* is responsible for alkane biosynthesis and is closely associated with biotic and abiotic stress responses (Aarts et al., 1995; Bourdenx et al., 2011; Bernard et al., 2012). For example, *CER1*-overexpressing transgenic plants showed reduced cuticle permeability and drought tolerance. However, these plants also had increased susceptibility to microbial pathogens (Bernard et al., 2012). Our results demonstrate that the

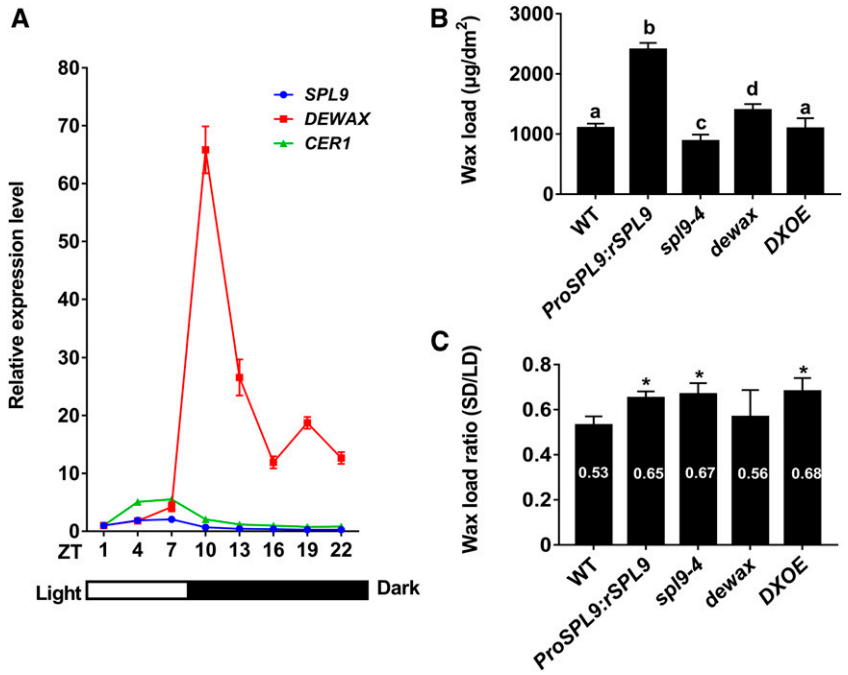

Figure 11. SPL9-DEWAX Is Involved in the Diurnal Regulation of Wax Synthesis.

(A) Diurnal expression of *CER1*, *SPL9*, and *DEWAX* genes in SD (8 h of light/16 h of dark) conditions. Gene expression was analyzed in 9-d-old Arabidopsis wild-type seedlings, which were grown under SD conditions. The light is on at Zeitgeber time 0 (ZT0) and off at ZT8. Total RNA was extracted from each sample (every 3 h from ZT1) and subjected to RT-qPCR analysis. Error bars indicate ±SD with at least three replicates, with each replicate containing at least 20 seedlings.

(B) Cuticular wax amounts of stems from ~3-month-old wild-type, *ProSPL9:rSPL9*, *spl9-4*, *dewax*, and *DXOE* plants grown in SD conditions. Cuticular waxes were extracted with hexane and analyzed by GC-FID. Wax coverage is expressed as wax amounts per stem surface area (μg.dm^{-2}). Error bars indicate ±SD from three replicate experiments with samples independently harvested on different days. Letters denote statistically significant differences between the indicated samples, as determined by ANOVA with post hoc Tukey Honestly Significant Difference.

(C) Total wax loads ratio between SD and LD conditions. Values from plants grown in SD conditions were divided by those from plants grown in LD conditions, and the data were analyzed using Student's *t* test (*P < 0.05). Error bars indicate ±SD from biological triplicate experiments.

miR156-SPL9 module directly regulates *CER1* expression and wax synthesis, primarily alkane synthesis. Microarray analysis or miRNA sequencing has provided evidence that miR156 expression is regulated by various abiotic stresses such as salt, drought, and cold (Sunkar and Zhu, 2004; Liu et al., 2008; Zhou et al., 2008; Lee et al., 2010) or biotic stresses (Joshi et al., 2016; Zhang et al., 2019). Yet, we do not know how miR156 perceives and responds to these environmental signals, and whether the miR156-SPL9-CER1 pathway defines a more commonly used or general stress response mechanism involved in plant tolerance to many other types of stress.

Transcriptional regulators of cuticle biosynthesis are classified mainly by several families of TFs including MYB and AP2/EREBP (Aharoni et al., 2004; Broun et al., 2004; Seo et al., 2011; Borisjuk et al., 2014). Our results here provide the first identification of a novel gene family, the SPLs in wax regulation. In plants, multiple SPLs are targeted by miR156s through cleavage and/or translational repression. In our results, the *spl9-4 spl15-1* double mutant showed a lower wax load than the *spl9* single mutant, and the *Pro35S:MIR156* transgenic line exhibited the lowest wax amounts, which illustrated that members of the SPL family may act redundantly, or otherwise have overlapping functions, in regulating wax synthetic responses. Therefore, further experiments to analyze the regulatory effects of other genes in the SPL family are needed for a better understanding of their roles in wax biosynthesis.

Besides some redundancy as indicated here, genes in the SPL family also have distinct functions (Xu et al., 2016). *SPL9* and *SPL15* are closely related homologs, and yet they exhibit distinct mRNA expression patterns (Wang et al., 2009; Hyun et al., 2016). Indeed, Arabidopsis gene expression analysis (http://bar.utoronto.ca/efp/cgi-bin/efpWeb.cgi) showed that the *SPL9* transcript level is approximately three- to ninefold higher than *SPL15* in epidermal stems, which is consistent with the more distinct wax defects exhibited by *spl9-4* and *spl15-1*. These results suggest that *SPL9* plays a larger role in epidermal wax synthesis than *SPL15*, perhaps determined by their different epidermal expression patterns. Furthermore, among the examined five SPL genes, only SPL9 could be shown to interact with DEWAX, which suggested that both gene expression and protein interaction difference led to SPL functional diversification from the other family members in wax synthesis regulation. Additionally, a recent paper demonstrated that there was a significant decrease in alkane levels in *DEWAX2* (a DEWAX homolog) overexpression leaves when compared with

the wild type (Kim et al., 2018). Whether DEWAX2 interacts with SPL9 remains to be determined.

Downstream Genes in Wax Synthesis Regulated by miR156-SPL9

In previous studies, transcription factors involved in wax regulation showed multiple targets (reviewed in Borisjuk et al., 2014; Lee and Suh, 2015a). However, there is no direct evidence or genetic analysis that reveals the causal relationship between these genes and those associated with wax synthesis. In this report, we examined a genetic line having one or more mutations, and transgenes, in various combinations to test the regulatory role of transcription factors on wax synthesis genes. The specific significance for a single wax component in cuticle function during environmental or developmental processes remains largely unknown. Because the cuticle wax synthesis pathways are tightly interconnected, it is challenging to examine the role of a single wax component using a loss of function approach (Goodwin et al., 2005). For example, in the *cer1-2* mutant, besides the alkanes, the amounts of 1-alcohols (primarily regulated by CER4) were also decreased (Supplemental Table 1). Through genetic approaches, we were able to uncouple the CER1 and CER4 synthesis pathway through overexpression of *SPL9*. In the *ProSPL9:rSPL9 cer1-2* line, the alkane contents were similar to *cer1-2*. However, the 1-alcohol contents were increased. Conversely, in the *ProSPL9:rSPL9 cer4-4* line, the 1-alcohol contents were similar to *cer4-4*, whereas the alkane contents were increased. It is of great interest to note that the *Pro35S:MIM156 cer4-4* and *ProSPL9:rSPL9 cer4-4* lines show a glossy phenotype as in some wax deficient mutants, although their total wax loads are higher than in wild-type plants. These results suggest that the different crystalline organization but not the total content of the waxes determines the appearance of the wax phenotype. This type of observation has also been reported in several other studies (Rowland et al., 2006; Pascal et al. , 2013, 2019; Haslam et al., 2015). In the *ProSPL9:rSPL9 cer1-2 cer4-4* line, both the alkane and 1-alcohol contents were decreased, similar to *cer1-2 cer4-4*. These unique genetic materials shed light on gene control over wax metabolism, and ultimate composition.

At the molecular level, we demonstrated that SPL9 directly regulated *CER1* expression, but also has a significant indirect effect on *CER4* expression. Although the promoter region of *CER4* contains a putative SPL9 binding cis-element, neither EMSA nor ChIP-qPCR experiments revealed SPL9 binding. Thus, the *CER4* promoter is likely not the immediate target of SPL9. Furthermore, it should be noted that almost all wax components in the stems of *ProSPL9:rSPL9* showed elevated levels in comparison with wild-type plants (Figure 2; Supplemental Table 1). Until now, at least tens of genes are reported to affect wax synthesis (Lee and Suh, 2015a). Although we did not examine all of the genes, it is possible that other wax synthesis-related genes are also differentially expressed in the mutant. In the future, systematic analysis of the transcriptome of the miR156-SPL9-related genetic materials may help identify the immediate transcription factor(s) governing the expression of *CER4* and other wax biosynthetic genes as potential SPL9 targets.

Potential Upstream Factors Regulate miR156-SPL9

We observed that SPL9 protein levels oscillated in a diurnal manner, with higher levels in the light and lower levels in the dark, respectively, and could be tied directly to the rhythmic synthesis of wax. By contrast, DEWAX accumulated in the dark (and inhibited wax synthesis) and decreased after light illumination. The upstream regulatory factors of miR156-SPL9 or DEWAX are unknown. Light/dark cycles influence photosynthesis, and ultimately sugar metabolism in plants. Indeed, sugar levels could regulate miR156 abundance, as reported by several groups (Wahl et al., 2013; Yang et al., 2013; Yu et al., 2013). The expression of miR156 was repressed by exogenous sugar treatment, leading to an increase in *SPL* gene expression and an early juvenile-adult phase transition (Yang et al., 2013; Yu et al., 2013). In accordance with this result, mutants with reduced endogenous sugars abundance showed increased miR156 expression and delayed phase transition (Yang et al., 2013; Yu et al., 2013). Another set of experiments demonstrated the role of trehalose 6-phosphate (T6P) in repressing miR156 expression during flowering (Wahl et al., 2013). T6P is considered to be a signaling molecule because it is present at low concentrations in plant cells. Therefore, further research will be necessary to investigate whether sugar or T6P regulates wax synthesis upstream of miR156.

As sessile organisms that rely on sunlight as the main source of energy, plants have developed sophisticated systems to sense and respond to light cues. Interestingly, light has been reported to control miRNA accumulation and their biological function at multiple layers, such as miRNA gene transcription, miRNA biogenesis, and RNA-induced silencing complex activity (Cho et al., 2014; Tsai et al., 2014; Sanchez-Retuerta et al., 2018). Recently, Xie et al. (2017) demonstrated that several PHYTOCHROME INTERACTING FACTORs (PIFs) directly bound to the promoters of five *MIR156* genes and repress their transcription. Their results established a direct link between the light–phytochrome–PIF pathways and miR156-SPL modules. Furthermore, it was shown that PIF4 integrates red light signaling and miRNA function through interacting with a miRNA biogenesis component DICER-LIKE1 and simultaneously regulates the expression of many miRNA genes during dark-to-red-light or red-light-to-dark transitions (Sun et al., 2018). Taken together, these data could provide a potential mechanistic explanation, at the molecular level, on how the diurnal light cycles might be involved in regulating the miR156-SPL module via genes involved in light signal transduction such as PIFs. The roles of such genes in wax synthesis await further investigation. It should also be noted that, in our results, we showed that even in *ProSPL9:rSPL9* plants, the diurnal expression of *SPL9* still exists (Figure 9), which may be independent of miR156. Thus, there may be an unknown direct regulator of *SPL9* during the light response.

Protein Interaction Regulation of SPL9 Activity

SPL9 has been known to be integrated into diverse developmental and metabolic pathways through either transcript cleavage or translational repression by miR156 at the posttranscriptional level. However, whether its protein activity is regulated by other factors remains to be fully elucidated. As shown by our EMSA results,

SPL9 specifically bound to the GTAC motifs in the *CER1* promoter. Furthermore, the binding of SPL9 to the GTAC motif was repressed when the DEWAX protein was present, demonstrating that the DNA binding ability of SPL9 protein could be regulated by DEWAX. Interestingly, previous studies found that although DEWAX acts as a repressor of wax biosynthetic genes, it does not contain the ERF-associated repression motif. Our results provide a molecular explanation of DEWAX-mediated transcriptional repression. This hypothesis is also supported by the transient transcription assays in tobacco, which showed the DEWAX sequestering activity of the SPL9 protein. Homo- or heterodimerization of SPL9 and DEWAX might regulate the target genes in response to the development and ever-changing environment. Similarly, protein activity regulation through heterodimerization has also been found in other light signal transduction pathways (Hornitschek et al., 2009; Hao et al., 2012). For example, atypical basic helix-loop-helix (bHLH) transcription factors, LONG HYPOCOTYL IN FAR-RED1 and PHY RAPIDLY REGULATED1, could directly interact with PIF4/PIF5, and pair with them to form a non-DNA binding heterodimer. This regulatory mechanism in plants may help to prevent an exaggerated response to shade, affording plants the flexibly to adapt to changeable light conditions. Alternatively, it should be noted that DEWAX and DEWAX2 transcription factors are able to bind directly to the canonical GCC or GCC-like motifs of the *CER1* promoter (Go et al., 2014; Kim et al., 2018). In our EMSA experiment, the DNA probes used contained no canonical GCC or GCC-like motifs, which preclude the possibility that DEWAX competes with SPL9 to bind the *CER1* promoter in vitro. However, we cannot exclude the possibility that the DEWAX-DNA interaction could compete with SPL9 and prevent its binding to the *CER1* promoter in vivo.

Working Model for SPL9-DEWAX Interaction

We report the regulation of SPL9 activity by the negative regulator DEWAX, and link diurnal cycles in plants to wax synthesis. DEWAX interferes with the formation of SPL9 homodimers by forming nonfunctional heterodimers with reduced DNA binding ability. If all these results together are considered, it is possible to propose a hypothetical model that explains the roles of SPL9 and DEWAX in mediating the diurnal regulation of wax synthesis (Figure 12). Under light conditions, SPL9 binds to GTAC motifs in the promoter of *CER1* to regulate alkane synthesis, but also indirectly increases *CER4* gene expression for 1-alcohol production through hitherto unknown mechanisms. Under dark conditions, DEWAX protein accumulates and competes with SPL9 to bind to the GTAC motifs present in the promoters of *CER1*, resulting in the downregulation of *CER1*. Our findings illustrate an elegant SPL9-DEWAX module that explains the antagonistic interactions between light and dark signaling pathways, ostensibly as a means to optimize wax synthesis in development and/or the environmental response in Arabidopsis.

In Arabidopsis, the total wax amount in the stems is over 10 times higher than that in the leaves (Suh et al. 2005), but the underlying mechanism of such organ-specific wax deposition remains unknown. Go et al. (2014) suggested that *DEWAX* may be responsible for the repression of wax biosynthesis in the leaves. In their study, the *DEWAX* expression levels were ~10- to 75-fold higher in leaves than in stems. Conversely, *SPL9* expression has been shown to be developmentally regulated, and to be higher in stems than in leaves (Wu et al., 2009). Thus, SPL9-DEWAX may function as a molecular switch in the integration of endogenous developmental cues and external signals, notably varying light levels, to coordinate plant development with epidermal wax synthesis.

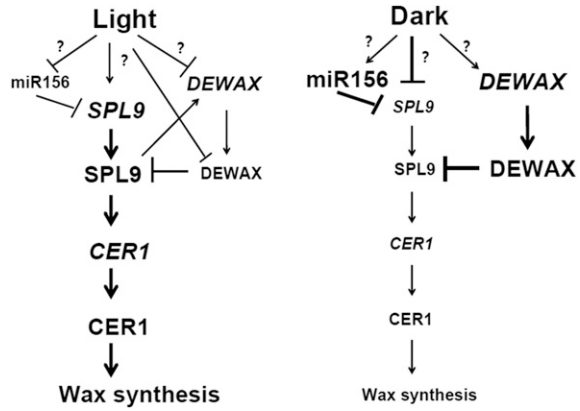

Figure 12. Proposed Working Model of the SPL9-DEWAX Signaling Module.

SPL9 and DEWAX gene and protein expression levels oscillated in a diurnal cycle, through multiple layers of transcriptional, posttranscriptional, and/or posttranslational regulations. During the day or in the light conditions, *SPL9* expression was transcriptionally activated in a miR156-resistant manner, and miR156 and *DEWAX* expressions were inhibited. SPL9 also upregulated *DEWAX* expression in the day, forming a negative feedback loop that may be important in moderating the light response in wax synthesis. Furthermore, DEWAX protein was degraded through the 26S proteasome-dependent pathway in the light. During the night or in the dark conditions, *miR56* and *DEWAX* expressions were induced and *SPL9* expression was repressed. Furthermore, DEWAX directly interacts with SPL9 to form a heterodimer and inhibit its DNA binding ability. The diurnal gene or protein expression of SPL9 and DEWAX, and SPL9 protein activity regulation by DEWAX may operate together to modulate *CER1* rhythmic gene expression and wax synthesis through the light/dark cycle.

METHODS

Plant Materials and Growth Conditions

All Arabidopsis (*Arabidopsis thaliana*) materials used in this study are of the *Columbia* (*Col-0*) genetic background. All plants were grown under long days (16-h light/8-h dark) at 23°C. The transgenic and mutant lines used in this study including *spl9-4 spl15-1*, *Pro35S:MIR156*, *Pro35S:MIM156*, *ProSPL9:rSPL9*, *ProSPL9:rSPL9-GR*, and *ProSPL9:GFP-rSPL9* were previously described by Gou et al. (2011), and were kindly provided by Dr. Jia-Wei Wang. The reporter lines *ProSPL9:SPL9-GUS* and *ProSPL9:rSPL9-GUS* (Xu et al., 2016) were supplied by Scott Poethig. *DXOE* and *dewax* were kind gifts from Mi Chung Suh. The T-DNA insertion mutants *spl9-4* (SAIL_150_B05), *spl15-1* (SALK_074426), *cer1-2* (SALK_014839), and *cer4-4* (SALK_000575) were obtained from the Arabidopsis Biological Resource Center (http://www.arabidopsis.org). For seedling experiments, seeds were sown on Murashige and Skoog agar medium containing 2% (w/v) Suc after surface sterilization and stratified at

4°C in the dark for 3 d. Then the seedlings were placed in a growth chamber and grown under white fluorescent light at light intensity of 100 μmol photons/m^2/s at 23°C (16-h light/8-h dark) for 7 d before further treatment. For DEX induction, 1-week-old seedlings were sprayed with 10 μM DEX plus 10 μM CHX, 10 μM DEX, or water (mock), respectively.

Cuticular Wax Analysis

The cuticular wax composition of leaves and stems of 6-week-old plants was determined as described by Lü et al. (2009).

Constructs and Plant Transformation

DNA constructs used in the study were generated based on construction methods following the classic molecular biology protocols and Gateway technology (Invitrogen). For Gateway cloning, all the gene sequences were cloned into the pDONR207 vector (Gateway) and subsequently introduced into certain destination vectors. To generate *Pro35S:HA-DEWAX* or *Pro35S:FLAG-rSPL9* fusion constructs, the coding DNA sequence of DEWAX or rSPL9 was cloned into pEarleyGate 201 or pEarleyGate 202, respectively. For *ProDEWAX:DEWAX-GUS* transgene, a genomic fragment spanning the 1.5-kb *DEWAX* promoter region upstream of the start codon and the *DEWAX* genomic region without stop codon was PCR amplified and cloned into the pMDC162 vector. For plant transformation, The pMDC162 harboring the *ProDEWAX:DEWAX-GUS* construct was introduced into *Agrobacterium tumefaciens* strain *GV3101* by the freeze-thaw method and further transformed into Arabidopsis plants using the floral dip method (Clough and Bent, 1998).

RNA Extraction and Quantitative RT-PCR

Total RNA was extracted with the Plant RNeasy Mini kit (Qiagen). About 1 μg of total RNA was DNase I treated and further used for reverse transcription with Moloney murine leukemia virus reverse transcriptase (Promega). The cDNA was diluted to 100 μL with water, and 1 μL of the diluted cDNA was used for RT-qPCR with the SYBR Premix ExTaq kit (Takara, Japan) in a total volume of 25 μL on the Applied Biosystems 7500 real-time PCR system according to the manufacturer's manual. The level of *PP2A* (*AT1G13320*) transcript was used as an internal control. The expression level of target genes are the ratio of expression in samples compared with the controls by the $2^{-\Delta\Delta Ct}$ method. All the experiments were performed independently three times. All the primers used are listed in Supplemental Table 3. For mature miR156, a stem loop RT-qPCR was performed according to a previous protocol (Varkonyi-Gasic et al., 2007).

Yeast One-Hybrid and Yeast Two-Hybrid Assay

For yeast one-hybrid assay, the coding regions of *SPL9* were PCR amplified and ligated to the pGADT7 vector (Clontech) to produce AD-SPL9, and a 1-kb promoter of *CER1* was cloned into the pHIS2 vector (Clontech) to produce pHIS2-*CER1*. For yeast two-hybrid assay, the coding regions of *DEWAX* and *SPL9* were PCR amplified from cDNAs and ligated to the pGADT7 and pGBKT7 vectors (Clontech) to generate pGADT7-DEWAX and pGBKT7-SPL9, respectively. Plasmids were co-transformed into yeast strain AH109 (Clontech) by the LiAc-PEG3350 method. Transformants were selected on SD-Leu-Trp plates. Interactions were tested on SD-Leu-Trp-His plates supplemented with 5 mM 3-amino-1,2,4,-triazole . Three independent clones for each transformation were tested.

ChIP-qPCR Assay

ChIP-qPCR assays was performed following the procedure described previously (Gou et al., 2011). About 2 g of harvested *ProSPL9:rSPL9-GFP* and the respective control (Col-0) samples were subjected to vacuum infiltration and cross-linked in fixation buffer [10 mM Tris–HCl (pH 8.0), 0.4 M Suc, 0.05% (v/v) Triton X-100, 1% (v/v) formaldehyde] for 10 min, followed by neutralization with 0.25 M Gly. Sonication was applied to break the genomic DNA into a size range from 200 to 1000 bp. Rabbit Anti-GFP antibody (use 5 μg antibody for 1 μg of chromatin, Abcam ChIP grade, ab290) and protein G plus agarose (Santa Cruz, sc-2002) were used for the immunoprecipitation. The cross-linking was reversed at 65°C overnight, and DNA was extracted. Finally, the GFP-specific enrichments of the fragments from *CER1* promoters were analyzed by qPCR with specific primers, as shown in Supplemental Table 3. The values were standardized to the input DNA to obtain the enrichment fold. All samples for ChIP were prepared with three biological replicates (samples independently harvested on different days).

BiFC Analysis

For the BiFC assays, the full-length *DEWAX* was fused with N-terminal YFP (*nYFP*), and *rSPL9* was fused with C-terminal YFP (*cYFP*; Walter et al., 2004). *A. tumefaciens* bacteria strain *GV3101* was transformed with the above vectors or control empty vector and then coinjected into young *Nicotiana benthamiana* leaves. Fluorescence signals were observed with confocal microscopy (Leica TCS SP8).

Co-IP Analysis

Co-IP assay was performed as previously described (Gou et al., 2011). *N. benthamiana* leaves were infiltrated with *A. tumefaciens* harboring *Pro35S:HA-DEWAX* or *Pro35S:FLAG-rSPL9* constructs.

Pull Down

To analyze in vitro protein interaction between SPL9 and DEWAX, *Escherichia coli BL21* (*DE3*) cells were transformed with *GST-DEWAX* and *6xHis-SPL9*, respectively. An *E.coli* strain expressing GST was used as a negative control. *E. coli* was cultivated overnight and then diluted 1:100 the next morning to grow another 3 h at 37°C. isopropyl β-D-1-thio-galactopyranoside (0.5 mM) was used to induce the expression of proteins at 16°C when the cells reached the logarithmic phase. Then the mixed 1 mL of *E. coli* (0.5 mL GST tagged plus 0.5 mL 6xHis tagged) cells were resuspended in phosphate buffered saline + Tween 20 and broken with a sonicator on ice. After centrifugation at 15,000 g for 30 min at 4°C, 20 μL nickel-nitrilotriacetic acid agarose (Bio-Rad) or glutathione-sepharose resin (GE Healthcare) was added to the supernatant mixture sample and rotated at 4°C for 3 h. The beads were washed with phosphate buffered saline + Tween 20 at least 4 times. Then SDS-PAGE gel-loading buffer was added to the beads and boiled for 5 min before electrophoresis. The protein was detected with anti-GST (Abmart M20007, 1/5000) or anti-6xHis (Abmart M30111, 1/5000) antibodies by immunoblot analysis.

Transient Transcription Dual-LUC Assays

For the Dual-LUC assays, the 1-kb promoter region of *CER1* was cloned into the pGreenII 0800-LUC vector (Hellens et al., 2005). The *Pro35S:rSPL9* or *ProCER1:LUC* constructs were introduced into *Agrobacterium tumefaciens* strain *GV3101*, and these *GV3101* cells harboring *Pro35S:rSPL9* or *ProCER1:LUC* were coinjected into *N. benthamiana* leaves and incubated at 25°C for 2 to 3 d. The

Pro35S:REN gene (*Renilla* luciferase) in the vector was used as an internal control. The ratio of firefly luciferase to *Renilla* luciferase (LUC/REN) was measured using a Dual-Luciferase Reporter Assay System (Promega) to reflect the activity of the promoter under various conditions.

SEM Analysis

Cryogenic SEM was used to view epicuticular wax crystallization patterns. Stem (second internode above the rosette) samples were collected from 6-week-old plants. Samples were prepared and viewed by cryo-SEM as described by Lü et al. (2009).

BiLC Assays

The BiLC assay was performed as described (Chen et al., 2008). The full-length or truncated forms of *SPL9* and *DEWAX* were cloned into pCAMBIA1300-nLUC or pCAMBIA1300-cLUC vector. *Agrobacterium tumefaciens* bacteria strain *GV3101* carrying different constructs was coinfiltrated into *N. benthamiana* leaves. After infiltration, plants were incubated under dark conditions for 12 h and then transferred to light conditions for 48 h. A low-light-cooled charge-coupled device imaging apparatus (LAS 4000 mini) was used to capture the LUC image. In each analysis, three independent leaves were infiltrated and analyzed, and three biological replications were performed by different transformations at different days with similar results.

Recombinant Protein Purification

The full-length coding region of *SPL9* or *DEWAX* was PCR amplified and cloned into the pGEX-2T vector (Amersham) to generate the pGEX-2T-SPL9 or pGEX-2T-DEWAX constructs, respectively. The plasmid was transformed into the *E. coli BL21* (*DE3*) strain. Expression of the fusion protein was induced by 0.5 mM IPTG and incubated at 16°C overnight. The fusion protein was purified using glutathione-sepharose resin (GE Healthcare).

EMSA

For EMSAs, two complementary 50-bp length oligonucleotides containing the GTAC motif of the *CER1* promoter were synthesized and labeled with biotin. Double strand DNA probes were obtained by annealing two complementary oligonucleotides. DNA gel mobility shift assay was performed using the EMSA kit (Beyotime) following the manufacturer's protocol.

GUS Assays

For histochemical GUS staining, seedlings were pretreated in 90% (v/v) acetone and then soaked and kept in the GUS staining buffer [50 mM sodium phosphate (pH = 7.2), 10 mM EDTA, 2.5 mM potassium ferricyanide, 2.5 mM potassium ferrocyanide, and 0.1% (v/v) Triton X-100] containing 1 mg/ml 5-bromo-4-chloro-3-indolylglucuronide at 37°C in darkness for 3 h. The stained seedlings were decolorized in 70% (v/v) ethanol and photographed using a SMZ25 dissecting microscope (Nikon). Results shown are representative of 3-6 individual plants. For quantifications of GUS protein levels, MUG activity was determined with a fluorescence spectrophotometer as previously described (Wu and Poethig, 2006).

Statistical Analyses

For statistical analysis, one-way analysis of variance (ANOVA) or Student's *t* test performed by GraphPad Prism 7.0 (GraphPad Software, www.graphpad.com) was used as specified in each figure and in Supplemental Data Set. Asterisks indicate statistical differences (*$P < 0.05$, **$P < 0.01$, ***$P < 0.001$). Different lowercase letters in the graphs indicate significant differences. Data represent mean values, and error bars are SD.

Accession Numbers

Sequence data from this article can be found in the *Arabidopsis* Genome Initiative database under the following accession numbers: *SPL3* (*AT2G33810*), *SPL4* (*AT1G53160*), *SPL5* (*AT3G15270*), *SPL9* (*At2g42200*), *SPL15* (*AT3G57920*), *DFR* (*At5g42800*), *DEWAX* (*At5g61590*), *CER1* (*At1g02205*), *CER3* (*At5g57800*), *CER4* (*At4g33790*), *CER5* (*AT1G51500*), *CER6* (*AT1G68530*), *CER10* (*AT3G55360*), *MIR156A* (*AT1G66783*), *MIR156C* (*AT4G31877*), *PP2A* (*At1g13320*).

Supplemental Data

Supplemental Figure 1. Cuticular wax amounts of leaves from 5-week-old wild-type, *Pro35S:MIR156*, *Pro35S:MIM156* and *SPL9* related Arabidopsis mutants grown in long day conditions.

Supplemental Figure 2. Cuticular wax compositions of leaves of wild-type, *Pro35S:MIR156*, *Pro35S:MIM156* and *SPL9* related Arabidopsis mutants grown in long day conditions.

Supplemental Figure 3. SEM images of epicuticular wax crystals on leaves of 5-week-old wild-type and *ProSPL9:rSPL9* plants grown in long-day conditions.

Supplemental Figure 4. RT-qPCR analysis of time course induction of *CER1* and *CER4* expression by dexamethasone (DEX) treatment in the *ProSPL9:rSPL9-GR* line.

Supplemental Figure 5. Glossy green and white waxy phenotypes of inflorescence stems of 6-week-old *ProSPL9:rSPL9 cer1-2*, *ProSPL9:rSPL9 cer4-4*, *Pro35S:MIM156 cer1-2* and *Pro35S:MIM156 cer4*-4 plants and their parents.

Supplemental Figure 6. Cuticular wax amounts of leaves from 5-week-old *ProSPL9:rSPL9 cer1-2*, *ProSPL9:rSPL9 cer4-4*, *Pro35S:MIM156 cer1-2*, *Pro35S:MIM156 cer4*-4 plants and their parents grown in long-day conditions.

Supplemental Figure 7. The N-terminal part of SPL9 and the N-terminal part of DEWAX contribute to their interaction.

Supplemental Figure 8. SPL9 and DEWAX protein interaction domain analysis in BiLC experiment.

Supplemental Figure 9. DEWAX represses the SPL9 transcriptional activity on the *CER4* promoter in the transient expression system.

Supplemental Figure 10. Diurnal expression of *pri-MIR156A*, *pri-MIR156C* and mature miR156.

Supplemental Figure 11. SPL9 directly regulates *DEWAX* expression.

Supplemental Figure 12. Light/dark changes altered expression of *pri-MIR156A*, *pri-MIR156C* and mature miR156.

Supplemental Table 1. Cuticular wax compositions in inflorescence stems of 6-week-old *ProSPL9:rSPL9 cer1-2*, *ProSPL9:rSPL9 cer4-4*, *Pro35S:MIM156 cer1-2* and *Pro35S:MIM156 cer4*-4 plants and their parents grown in long day conditions.

Supplemental Table 2. Cuticular wax compositions in leaves of 5-week-old *ProSPL9:rSPL9 cer1-2*, *ProSPL9:rSPL9 cer4-4*,

Pro35S:MIM156 cer1-2 and *Pro35S:MIM156 cer4*-4 plants and their parents grown in long day conditions.

Supplemental Table 3. Primers used in this study.

Supplemental Data Set. Summary of statistical tests.

ACKNOWLEDGMENTS

We thank Jia-Wei Wang (Shanghai Institutes for Biological Sciences), Mi Chung Suh (Chonnam National University), and Scott Poethig (University of Pennsylvania) for providing us with the seeds. This work was supported by the National Natural Science Foundation of China (NSFC) (31570186 to S.L. and 31400276 to R.-J.L.).

AUTHOR CONTRIBUTIONS

R.-J.L., L.-M.L., and S.L. designed the research; R.-J.L., L.-M.L., X.-L.L., and J.-C.K. performed the experiments and analyzed the data; R.-J.L., M.A.J., and S.L. wrote the article.

Received April 2, 2019; revised August 12, 2019; accepted August 30, 2019; published September 4, 2019.

REFERENCES

Aarts, M.G., Keijzer, C.J., Stiekema, W.J., and Pereira, A. (1995). Molecular characterization of the *CER1* gene of *Arabidopsis* involved in epicuticular wax biosynthesis and pollen fertility. Plant Cell **7:** 2115–2127.

Aharoni, A., Dixit, S., Jetter, R., Thoenes, E., van Arkel, G., and Pereira, A. (2004). The *SHINE* clade of AP2 domain transcription factors activates wax biosynthesis, alters cuticle properties, and confers drought tolerance when overexpressed in *Arabidopsis*. Plant Cell **16:** 2463–2480.

Baker, E.A. (1974). The Influence of environment on leaf wax development in *Brassica Oleracea Var. Gemmifera*. New Phytol. **73:** 955–966.

Bernard, A., Domergue, F., Pascal, S., Jetter, R., Renne, C., Faure, J.D., Haslam, R.P., Napier, J.A., Lessire, R., and Joubes, J. (2012). Reconstitution of plant alkane biosynthesis in yeast demonstrates that *Arabidopsis ECERIFERUM1* and *ECERIFERUM3* are core components of a very-long-chain alkane synthesis complex. Plant Cell **24:** 3106–3118.

Bernard, A., and Joubès, J. (2013). *Arabidopsis* cuticular waxes: Advances in synthesis, export and regulation. Prog. Lipid Res. **52:** 110–129.

Borges, F., and Martienssen, R.A. (2015). The expanding world of small RNAs in plants. Nat. Rev. Mol. Cell Biol. **16:** 727–741.

Borisjuk, N., Hrmova, M., and Lopato, S. (2014). Transcriptional regulation of cuticle biosynthesis. Biotechnol. Adv. **32:** 526–540.

Bourdenx, B., Bernard, A., Domergue, F., Pascal, S., Leger, A., Roby, D., Pervent, M., Vile, D., Haslam, R.P., Napier, J.A., Lessire, R., and Joubes, J. (2011). Overexpression of *Arabidopsis ECERIFERUM1* promotes wax very-long-chain alkane biosynthesis and influences plant response to biotic and abiotic stresses. Plant Physiol. **156:** 29–45.

Broun, P., Poindexter, P., Osborne, E., Jiang, C.Z., and Riechmann, J.L. (2004). *WIN1*, a transcriptional activator of epidermal wax accumulation in *Arabidopsis*. Proc. Natl. Acad. Sci. USA **101:** 4706–4711.

Cardon, G., Hohmann, S., Klein, J., Nettesheim, K., Saedler, H., and Huijser, P. (1999). Molecular characterisation of the *Arabidopsis* SBP-box genes. Gene **237:** 91–104.

Chen, X., Goodwin, S.M., Boroff, V.L., Liu, X., and Jenks, M.A. (2003). Cloning and characterization of the *WAX2* gene of *Arabidopsis* involved in cuticle membrane and wax production. Plant Cell **15:** 1170–1185.

Chen, H., Zou, Y., Shang, Y., Lin, H., Wang, Y., Cai, R., Tang, X., and Zhou, J.M. (2008). Firefly luciferase complementation imaging assay for protein-protein interactions in plants. Plant Physiol. **146:** 368–376.

Cho, S.K., Ben Chaabane, S., Shah, P., Poulsen, C.P., and Yang, S.W. (2014). *COP1* E3 ligase protects *HYL1* to retain microRNA biogenesis. Nat. Commun. **5:** 5867.

Chuck, G., Cigan, A.M., Saeteurn, K., and Hake, S. (2007). The heterochronic maize mutant *Corngrass1* results from overexpression of a tandem microRNA. Nat. Genet. **39:** 544–549.

Clough, S.J., and Bent, A.F. (1998). Floral dip: A simplified method for *Agrobacterium*-mediated transformation of *Arabidopsis thaliana*. Plant J. **16:** 735–743.

Cui, L.G., Shan, J.X., Shi, M., Gao, J.P., and Lin, H.X. (2014). The *miR156–SPL9-DFR* pathway coordinates the relationship between development and abiotic stress tolerance in plants. Plant J. **80:** 1108–1117.

Franco-Zorrilla, J.M., Valli, A., Todesco, M., Mateos, I., Puga, M.I., Rubio-Somoza, I., Leyva, A., Weigel, D., García, J.A., and Paz-Ares, J. (2007). Target mimicry provides a new mechanism for regulation of microRNA activity. Nat. Genet. **39:** 1033–1037.

Gandikota, M., Birkenbihl, R.P., Hohmann, S., Cardon, G.H., Saedler, H., and Huijser, P. (2007). The *miRNA156/157* recognition element in the 3′ UTR of the *Arabidopsis* SBP box gene *SPL3* prevents early flowering by translational inhibition in seedlings. Plant J. **49:** 683–693.

Giese, B.N. (1975). Effects of light and temperature on the composition of epicuticular wax of barley leaves. Phytochemistry **14:** 921–929.

Go, Y.S., Kim, H., Kim, H.J., and Suh, M.C. (2014). *Arabidopsis* cuticular wax biosynthesis is negatively regulated by the *DEWAX* gene encoding an AP2/ERF-type transcription factor. Plant Cell **26:** 1666–1680.

Goodwin, S.M., Rashotte, A.M., Rahman, M., Feldmann, K.A., and Jenks, M.A. (2005). Wax constituents on the inflorescence stems of double eceriferum mutants in *Arabidopsis* reveal complex gene interactions. Phytochemistry **66:** 771–780.

Gou, J.Y., Felippes, F.F., Liu, C.J., Weigel, D., and Wang, J.W. (2011). Negative regulation of anthocyanin biosynthesis in *Arabidopsis* by a miR156-targeted SPL transcription factor. Plant Cell **23:** 1512–1522.

Guo, A.Y., Zhu, Q.H., Gu, X., Ge, S., Yang, J., and Luo, J. (2008). Genome-wide identification and evolutionary analysis of the plant specific SBP-box transcription factor family. Gene **418:** 1–8.

Hannoufa, A., Negruk, V., Eisner, G., and Lemieux, B. (1996). The *CER3* gene of *Arabidopsis thaliana* is expressed in leaves, stems, roots, flowers and apical meristems. Plant J. **10:** 459–467.

Hao, Y., Oh, E., Choi, G., Liang, Z., and Wang, Z.Y. (2012). Interactions between HLH and bHLH factors modulate light-regulated plant development. Mol. Plant **5:** 688–697.

Haslam, T.M., Haslam, R., Thoraval, D., Pascal, S., Delude, C., Domergue, F., Fernández, A.M., Beaudoin, F., Napier, J.A., Kunst, L., and Joubès, J. (2015). *ECERIFERUM2-LIKE* proteins have unique biochemical and physiological functions in very-long-chain fatty acid elongation. Plant Physiol. **167:** 682–692.

Hooker, T.S., Millar, A.A., and Kunst, L. (2002). Significance of the expression of the *CER6* condensing enzyme for cuticular wax production in *Arabidopsis*. Plant Physiol. **129:** 1568–1580.

Hellens, R.P., Allan, A.C., Friel, E.N., Bolitho, K., Grafton, K., Templeton, M.D., Karunairetnam, S., Gleave, A.P., and Laing, M.A. (2005). Transient expression vectors for functional genomics, quantification of promoter activity and RNA silencing in plants. Plant Methods **1:** 13.

Hooker, T.S., Lam, P., Zheng, H., and Kunst, L. (2007). A core subunit of the RNA-processing/degrading exosome specifically influences cuticular wax biosynthesis in *Arabidopsis*. Plant Cell **19:** 904–913.

Hornitschek, P., Lorrain, S., Zoete, V., Michielin, O., and Fankhauser, C. (2009). Inhibition of the shade avoidance response by formation of non-DNA binding bHLH heterodimers. EMBO J. **28:** 3893–3902.

Hyun, Y., Richter, R., Vincent, C., Martinez-Gallegos, R., Porri, A., and Coupland, G. (2016). Multi-layered regulation of *SPL15* and cooperation with *SOC1* integrate endogenous flowering pathways at the *Arabidopsis* shoot meristem. Dev. Cell **37:** 254–266.

Jenks, M.A., Rich, P.J., and Ashworth, E.N. (1994). Involvement of cork cells in synthesis and secretion of filamentous epicuticular wax on *Sorghum bicolor (L.) Moench*. Int. J. Plant Sci. **155:** 506–518.

Jenks, M.A., Tuttle, H.A., Eigenbrode, S.D., and Feldmann, K.A. (1995). Leaf Epicuticular Waxes of the Eceriferum Mutants in Arabidopsis. Plant physiology **108:** 369–377.

Joshi, R.K., Megha, S., Basu, U., Rahman, M.H., and Kav, N.N. (2016). Genome wide identification and functional prediction of long non-coding RNAs responsive to *Sclerotinia sclerotiorum* infection in *Brassica napus*. PLoS One **11:** e0158784.

Kim, H., Go, Y.S., and Suh, M.C. (2018). *DEWAX2* transcription factor negatively regulates cuticular wax biosynthesis in *Arabidopsis* leaves. Plant Cell Physiol. **59:** 966–977.

Klein, J., Saedler, H., and Huijser, P. (1996). A new family of DNA binding proteins includes putative transcriptional regulators of the *Antirrhinum majus* floral meristem identity gene *SQUAMOSA*. Mol. Gen. Genet. **250:** 7–16.

Lam, P., Zhao, L., Eveleigh, N., Yu, Y., Chen, X., and Kunst, L. (2015). The exosome and trans-acting small interfering RNAs regulate cuticular wax biosynthesis during *Arabidopsis* inflorescence stem development. Plant Physiol. **167:** 323–336.

Lam, P., Zhao, L., McFarlane, H.E., Aiga, M., Lam, V., Hooker, T.S., and Kunst, L. (2012). *RDR1* and *SGS3*, components of RNA-mediated gene silencing, are required for the regulation of cuticular wax biosynthesis in developing inflorescence stems of *Arabidopsis*. Plant Physiol. **159:** 1385–1395.

Lee, S.B., and Suh, M.C. (2015a). Advances in the understanding of cuticular waxes in *Arabidopsis thaliana* and crop species. Plant Cell Rep. **34:** 557–572.

Lee, S.B., and Suh, M.C. (2015b). Cuticular wax biosynthesis is up-regulated by the *MYB94* transcription factor in *Arabidopsis*. Plant Cell Physiol. **56:** 48–60.

Lee, H., Yoo, S.J., Lee, J.H., Kim, W., Yoo, S.K., Fitzgerald, H., Carrington, J.C., and Ahn, J.H. (2010). Genetic framework for flowering-time regulation by ambient temperature-responsive miRNAs in *Arabidopsis*. Nucleic Acids Res. **38:** 3081–3093.

Li, F., Wu, X., Lam, P., Bird, D., Zheng, H., Samuels, L., Jetter, R., and Kunst, L. (2008). Identification of the wax ester synthase/acyl-coenzyme A: Diacylglycerol acyltransferase *WSD1* required for stem wax ester biosynthesis in *Arabidopsis*. Plant Physiol. **148:** 97–107.

Liu, H.H., Tian, X., Li, Y.J., Wu, C.A., and Zheng, C.C. (2008). Microarray-based analysis of stress-regulated microRNAs in *Arabidopsis thaliana*. RNA **14:** 836–843.

Lü, S., Song, T., Kosma, D.K., Parsons, E.P., Rowland, O., and Jenks, M.A. (2009). *Arabidopsis CER8* encodes *LONG-CHAIN ACYL-COA SYNTHETASE 1* (*LACS1*) that has overlapping functions with *LACS2* in plant wax and cutin synthesis. Plant J. **59:** 553–564.

Mitsuda, N., Ikeda, M., Takada, S., Takiguchi, Y., Kondou, Y., Yoshizumi, T., Fujita, M., Shinozaki, K., Matsui, M., and Ohme-Takagi, M. (2010). Efficient yeast one-/two-hybrid screening using a library composed only of transcription factors in *Arabidopsis thaliana*. Plant Cell Physiol. **51:** 2145–2151.

Nawrath, C., Schreiber, L., Franke, R.B., Geldner, N., Reina-Pinto, J.J., and Kunst, L. (2013). Apoplastic diffusion barriers in *Arabidopsis*. The Arabidopsis Book **11:** e0167.

Oshima, Y., Shikata, M., Koyama, T., Ohtsubo, N., Mitsuda, N., and Ohme-Takagi, M. (2013). *MIXTA*-like transcription factors and *WAX INDUCER1/SHINE1* coordinately regulate cuticle development in *Arabidopsis* and *Torenia fournieri*. Plant Cell **25:** 1609–1624.

Park, C.S., Go, Y.S., and Suh, M.C. (2016). Cuticular wax biosynthesis is positively regulated by *WRINKLED4*, an AP2/ERF-type transcription factor, in *Arabidopsis* stems. Plant J. **88:** 257–270.

Pascal, S., Bernard, A., Sorel, M., Pervent, M., Vile, D., Haslam, R.P., Napier, J.A., Lessire, R., Domergue, F., and Joubès, J. (2013). The *Arabidopsis cer26* mutant, like the *cer2* mutant, is specifically affected in the very long chain fatty acid elongation process. Plant J. **73:** 733–746.

Pascal, S., Bernard, A., Deslous, P., Gronnier, J., Fournier-Goss, A., Domergue, F., Rowland, O., and Joubès, J. (2019). *Arabidopsis CER1-LIKE1* functions in a cuticular very-long-chain alkane-forming complex. Plant Physiol. **179:** 415–432.

Pighin, J.A., Zheng, H., Balakshin, L.J., Goodman, I.P., Western, T.L., Jetter, R., Kunst, L., and Samuels, A.L. (2004). Plant cuticular lipid export requires an ABC transporter. Science **306:** 702–704.

Raffaele, S., Vailleau, F., Leger, A., Joubes, J., Miersch, O., Huard, C., Blee, E., Mongrand, S., Domergue, F., and Roby, D. (2008). A MYB transcription factor regulates very-long-chain fatty acid biosynthesis for activation of the hypersensitive cell death response in *Arabidopsis*. Plant Cell **20:** 752–767.

Rowland, O., Lee, R., Franke, R., Schreiber, L., and Kunst, L. (2007). The *CER3* wax biosynthetic gene from *Arabidopsis thaliana* is allelic to *WAX2/YRE/FLP1*. FEBS Lett. **581:** 3538–3544.

Rowland, O., Zheng, H., Hepworth, S.R., Lam, P., Jetter, R., and Kunst, L. (2006). *CER4* encodes an alcohol-forming fatty acyl-coenzyme A reductase involved in cuticular wax production in *Arabidopsis*. Plant Physiol. **142:** 866–877.

Rubio-Somoza, I., Zhou, C.M., Confraria, A., Martinho, C., von Born, P., Baena-Gonzalez, E., Wang, J.W., and Weigel, D. (2014). Temporal control of leaf complexity by miRNA-regulated licensing of protein complexes. Curr. Biol. **24:** 2714–2719.

Samad, A.F.A., Sajad, M., Nazaruddin, N., Fauzi, I.A., Murad, A.M.A., Zainal, Z., and Ismail, I. (2017). MicroRNA and transcription factor: Key players in plant regulatory network. Front. Plant Sci. **8:** 565.

Samuels, L., Kunst, L., and Jetter, R. (2008). Sealing plant surfaces: Cuticular wax formation by epidermal cells. Annu. Rev. Plant Biol. **59:** 683–707.

Sanchez-Retuerta, C., Suarez-Lopez, P., and Henriques, R. (2018). Under a new light: Regulation of light-dependent pathways by non-coding RNAs. Front. Plant Sci. **9:** 962.

Seo, P.J., Lee, S.B., Suh, M.C., Park, M.J., Go, Y.S., and Park, C.M. (2011). The *MYB96* transcription factor regulates cuticular wax biosynthesis under drought conditions in *Arabidopsis*. Plant Cell **23:** 1138–1152.

Shepherd, T., and Wynne Griffiths, D. (2006). The effects of stress on plant cuticular waxes. New Phytol. **171:** 469–499.

Shepherd, T., Robertson, G.W., Griffiths, D.W., Birch, A.N.E., and Duncan, G. (1995). Effects of environment on the composition of epicuticular wax from kale and swede. Phytochemistry **40:** 407–417.

Suh, M.C., Samuels, A.L., Jetter, R., Kunst, L., Pollard, M., Ohlrogge, J., and Beisson, F. (2005). Cuticular lipid composition, surface structure, and gene expression in *Arabidopsis* stem epidermis. Plant Physiol. **139:** 1649–1665.

Sun, Z., Li, M., Zhou, Y., Guo, T., Liu, Y., Zhang, H., and Fang, Y. (2018). Coordinated regulation of *Arabidopsis* microRNA biogenesis and red light signaling through *Dicer-like 1* and *phytochrome-interacting factor 4*. PLoS Genet. **14:** e1007247.

Sunkar, R., and Zhu, J.K. (2004). Novel and stress-regulated microRNAs and other small RNAs from *Arabidopsis*. Plant Cell **16:** 2001–2019.

Tsai, H.L., Li, Y.H., Hsieh, W.P., Lin, M.C., Ahn, J.H., and Wu, S.H. (2014). *HUA ENHANCER1* is involved in posttranscriptional regulation of positive and negative regulators in *Arabidopsis* photomorphogenesis. Plant Cell **26:** 2858–2872.

Varkonyi-Gasic, E., Wu, R., Wood, M., Walton, E.F., and Hellens, R.P. (2007). Protocol: A highly sensitive RT-PCR method for detection and quantification of microRNAs. Plant Methods **3:** 12.

Wahl, V., Ponnu, J., Schlereth, A., Arrivault, S., Langenecker, T., Franke, A., Feil, R., Lunn, J.E., Stitt, M., and Schmid, M. (2013). Regulation of flowering by trehalose-6-phosphate signaling in *Arabidopsis thaliana*. Science **339:** 704–707.

Walter, M., Chaban, C., Schütze, K., Batistic, O., Weckermann, K., Blazevic, D., Grefen, C., Schumacher, K., Oecking, C., Harter, K., and Kudla, J. (2004). Visualization of protein interactions in living plant cells using bimolecular fluorescence complementation. Plant J. **40:** 428–438.

Wang, J.W., Schwab, R., Czech, B., Mica, E., and Weigel, D. (2008). Dual effects of miR156-targeted SPL genes and CYP78A5/KLUH on plastochron length and organ size in *Arabidopsis thaliana*. Plant Cell **20:** 1231–1243.

Wang, J.W., Czech, B., and Weigel, D. (2009). miR156-regulated SPL transcription factors define an endogenous flowering pathway in *Arabidopsis thaliana*. Cell **138:** 738–749.

Wang, J.W., Park, M.Y., Wang, L.J., Koo, Y., Chen, X.Y., Weigel, D., and Poethig, R.S. (2011). miRNA control of vegetative phase change in trees. PLoS Genet. **7:** e1002012.

Wu, G., and Poethig, R.S. (2006). Temporal regulation of shoot development in *Arabidopsis thaliana* by miR156 and its target SPL3. Development **133:** 3539–3547.

Wu, G., Park, M.Y., Conway, S.R., Wang, J.W., Weigel, D., and Poethig, R.S. (2009). The sequential action of miR156 and miR172 regulates developmental timing in *Arabidopsis*. Cell **138:** 750–759.

Xie, Y., Liu, Y., Wang, H., Ma, X., Wang, B., Wu, G., and Wang, H. (2017). Phytochrome-interacting factors directly suppress *MIR156* expression to enhance shade-avoidance syndrome in *Arabidopsis*. Nat. Commun. **8:** 348.

Xu, M., Hu, T., Zhao, J., Park, M.Y., Earley, K.W., Wu, G., Yang, L., and Poethig, R.S. (2016). Developmental functions of miR156-Regulated *SQUAMOSA PROMOTER BINDING PROTEIN-LIKE* (*SPL*) genes in *Arabidopsis thaliana*. PLoS Genet. **12:** e1006263.

Yamasaki, H., Hayashi, M., Fukazawa, M., Kobayashi, Y., and Shikanai, T. (2009). SQUAMOSA Promoter Binding Protein-Like7 Is a Central Regulator for Copper Homeostasis in Arabidopsis. Plant Cell **21:** 347–361.

Yang, L., Xu, M., Koo, Y., He, J., and Poethig, R.S. (2013). Sugar promotes vegetative phase change in *Arabidopsis thaliana* by repressing the expression of *MIR156A* and *MIR156C*. eLife **2:** e00260.

Yu, N., Niu, Q.W., Ng, K.H., and Chua, N.H. (2015a). The role of miR156/SPLs modules in *Arabidopsis* lateral root development. Plant J. **83:** 673–685.

Yu, Z.X., Wang, L.J., Zhao, B., Shan, C.M., Zhang, Y.H., Chen, D.F., and Chen, X.Y. (2015b). Progressive regulation of sesquiterpene biosynthesis in *Arabidopsis* and *Patchouli* (*Pogostemon cablin*) by the miR156-targeted *SPL* transcription factors. Mol. Plant **8:** 98–110.

Yu, S., Cao, L., Zhou, C.M., Zhang, T.Q., Lian, H., Sun, Y., Wu, J., Huang, J., Wang, G., and Wang, J.W. (2013). Sugar is an endogenous cue for juvenile-to-adult phase transition in plants. eLife **2:** e00269.

Zhang, Q., Zhang, Y., Wang, S., Hao, L., Wang, S., Xu, C., Jiang, F., and Li, T. (2019). Characterization of genome-wide microRNAs and their roles in development and biotic stress in pear. Planta **249:** 693–707.

Zheng, H., Rowland, O., and Kunst, L. (2005). Disruptions of the *Arabidopsis* Enoyl-CoA reductase gene reveal an essential role for very-long-chain fatty acid synthesis in cell expansion during plant morphogenesis. Plant Cell **17:** 1467–1481.

Zhou, X., Wang, G., Sutoh, K., Zhu, J.K., and Zhang, W. (2008). Identification of cold-inducible microRNAs in plants by transcriptome analysis. Biochim. Biophys. Acta **1779:** 780–788.